

MissBench: Benchmarking Multimodal Affective Analysis under Imbalanced Missing Modalities

Tien Anh Pham

VNU University of Engineering and Technology
Hanoi, Vietnam
23021696@vnu.edu.vn

Duc-Trong Le

VNU University of Engineering and Technology
Hanoi, Vietnam
trongld@vnu.edu.vn

Phuong-Anh Nguyen

VNU University of Engineering and Technology
Hanoi, Vietnam
22028332@vnu.edu.vn

Cam-Van Thi Nguyen*

VNU University of Engineering and Technology
Hanoi, Vietnam
vanntc@vnu.edu.vn

Abstract

Multimodal affective computing underpins key tasks such as sentiment analysis and emotion recognition. Standard evaluations, however, often assume that textual, acoustic, and visual modalities are equally available. In real applications, some modalities are systematically more fragile or expensive, creating imbalanced missing rates and training biases that task-level metrics alone do not reveal. We introduce MissBench, a benchmark and framework for multimodal affective tasks that standardizes both shared and imbalanced missing-rate protocols on four widely used sentiment and emotion datasets. MissBench also defines two diagnostic metrics. The Modality Equity Index (MEI) measures how fairly different modalities contribute across missing-modality configurations. The Modality Learning Index (MLI) quantifies optimization imbalance by comparing modality-specific gradient norms during training, aggregated across modality-related modules. Experiments on representative method families show that models that appear robust under shared missing rates can still exhibit marked modality inequity and optimization imbalance under imbalanced conditions. These findings position MissBench, together with MEI and MLI, as practical tools for stress-testing and analyzing multimodal affective models in realistic incomplete-modality settings. For reproducibility, we release our code at: <https://anonymous.4open.science/r/MissBench-4098/>

CCS Concepts

• **Information systems** → **Multimedia information systems**; • **Computing methodologies** → **Simulation evaluation**; **Learning paradigms**.

Keywords

Multimodal affective computing, Imbalanced missing modalities, Modality equity, Gradient dominance

1 Introduction

Multimodal affective computing underpins key applications such as sentiment analysis and emotion recognition in dialog systems, call centers, and social media [7, 22, 39]. These systems typically integrate language, visual, and acoustic modalities, yet in realistic environments data from some modalities are often missing or

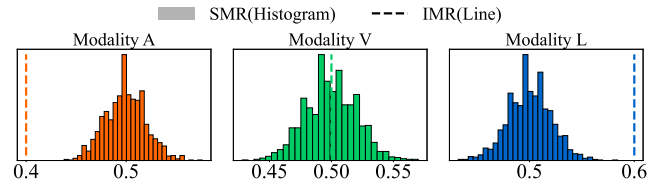


Figure 1: Sampled modality-specific missing rate under mean-match $SMR=0.5$ and $IMR=(0.4, 0.5, 0.6)$. Under SMR $r_m \approx r_{sh}$, while under IMR r_m can receive any predefined value $\in [0, 1)$.

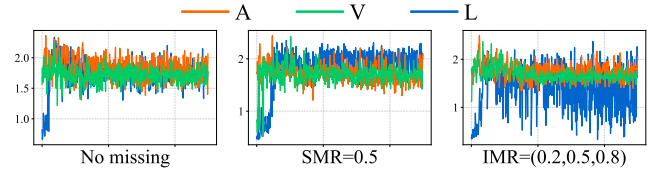


Figure 2: Decoupled modality parameters [28] of RedCore [25] on IEMOCAP under different missing-rate configurations, illustrating how a single dominant modality can drive most parameter updates under imbalanced missing rates.

severely degraded due to sensor failures, noise, occlusion, or privacy and transcription constraints [30, 37]. As a result, learning from incomplete multimodal inputs is essential for building reliable affective models [13, 14, 16].

A large body of work has been devoted to improving robustness under missing modalities, including imputation strategies, reconstruction-based models, and architectures designed to operate on arbitrary modality subsets [10, 17, 23, 40]. While these methods substantially improve performance compared to naive fusion, their evaluation predominantly relies on task-level metrics such as Accuracy, F1-score, MAE, or correlation. Such aggregate metrics summarize end performance but offer limited insight into *how* different modalities contribute, or how learning dynamics change when missingness is systematic rather than random [16, 29, 30].

In practice, missingness is rarely symmetric across modalities. Some modalities are systematically more fragile or costly than others. Audio channels may fail more frequently than text transcripts. In medical or sensor-rich scenarios, high-cost modalities

*Corresponding author.

Table 1: Comparison with prior work on missing modalities, multimodal imbalance, and benchmarks. “Missing protocol” shows whether SMR or IMR is explicitly modeled. “Mod.-level” and “Grad.-level” indicate modality-wise and optimization-level diagnostics comparable to odality Equity Index (MEI) and Modality Learning Index (MLI).

Work	Affective focus	Missing protocol	IMR (imb.)	Mod.-level diagnostics	Grad.-level diagnostics	Public benchmark
MMIN [40]	✓	SMR / pattern	×	×	×	×
GCNet [10]	✓	SMR / fixed	×	×	×	×
RedCore [25]	✓	IMR (custom)	✓	limited	×	×
MCE [38]	general	IMR (general)	✓	utility metric	gradient-aware	×
MultiBench [12]	mixed	noise / drop	×	×	×	✓
MERBench [11]	✓	noise / robustness	×	×	×	✓
MissMAC-Bench [15]	✓	fixed & random MR	×	perf. mean & std	×	✓
BalanceBenchmark [31]	general	imbalance	×	imbalance index	×	✓
MissBench (ours)	✓	SMR & IMR	✓	MEI	MLI	✓

may only be available for a small fraction of samples [25, 37, 38]. This leads to *imbalanced missing rates* (IMR), where certain modalities are observed much more often than others. IMR changes the effective exposure of each modality during training. As a result, learning can become biased toward dominant modalities. Under IMR, a single modality may receive a disproportionate share of gradient updates. This effect can produce biased representations even when task accuracy remains high [25, 29, 38]. Figure 1 illustrates the difference between shared missing rates (SMR) and IMR at the data level. Under SMR, all modalities exhibit similar empirical missing rates. Under IMR, modality-specific exposure differs substantially, even when the average missing rate is matched. Figure 2 shows a complementary effect at the optimization level. Using RedCore [25] as a representative IMR-aware method on IEMOCAP, the figure demonstrates that, under IMR conditions, the language modality consistently drives larger parameter updates than the visual and acoustic modalities. This observation indicates that IMR can induce persistent gradient dominance within the model. Importantly, this behavior is not revealed by task metrics alone. Although several recent methods explicitly consider IMR [24, 25, 38], many missing-modality handling approaches still assume shared or nearly symmetric missing patterns across modalities [6, 10, 27, 40]. More broadly, existing evaluations rarely distinguish SMR from IMR in a systematic manner. They also lack standardized tools for modality- and optimization-level analysis across missingness regimes.

At the benchmark level, prior efforts such as MultiBench [12] and multimodal affective benchmarks [15, 30] provide unified evaluation platforms but primarily focus on balanced or fixed corruption scenarios. As a result, current benchmarks mainly answer how accurate a model is under missing modalities. They offer limited insight into which modality is disadvantaged or how strongly each modality influences the optimization process. No existing benchmark simultaneously distinguishes shared and imbalanced missing-rate regimes and provides modality-aware diagnostics beyond task performance. In realistic deployments, however, imbalanced missing rates are common, making such analysis necessary.

To address this gap, we introduce **MissBench**, a benchmark and framework for incomplete multimodal affective computing that explicitly accounts for both shared and imbalanced missing rates.

MissBench reorganizes three English datasets (CMU-MOSI [34], CMU-MOSEI [35], and IEMOCAP [2]) and one Chinese dataset (CH-SIMS [33]) under controlled masking protocols that cover SMR and a family of IMR settings. Beyond conventional task metrics, we propose two diagnostic measures. The *Modality Equity Index* (MEI) quantifies how evenly different modalities contribute to predictive performance across missing-modality configurations. The *Modality Learning Index* (MLI) captures optimization imbalance by summarizing modality-specific gradient dynamics during training. MissBench exposes modality inequity and optimization dominance that remain hidden when evaluation is limited to task-level metrics. Overall, our main contributions are:

- We present **MissBench**, a benchmark for multimodal affective computing under incomplete modalities that standardizes shared and imbalanced missing-rate protocols on multiple datasets with fixed data splits and masking seeds for reproducible evaluation.
- We introduce two diagnostic metrics, the **Modality Equity Index** (MEI) and the **Modality Learning Index** (MLI), which quantify modality-level contribution equity and optimization imbalance from performance shifts and modality-specific gradient dynamics.
- We provide a unified evaluation pipeline and conduct a comprehensive empirical study across representative model families, showing that MissBench reveals modality inequity and optimization imbalance that are not captured by task metrics alone.

2 Related Work

Multimodal affective computing and robustness. Multimodal affective computing has been extensively studied, with surveys summarizing advances in feature design, fusion strategies, and robustness to noise and distribution shifts [2, 7, 34, 35]. These works primarily aim to improve task performance under clean or mildly corrupted inputs. When missing data are considered, they are typically treated as a secondary robustness factor rather than a central design axis. As a result, robustness is often assessed only at the output level. Modality-level contribution and optimization behavior remain largely unexplored in these studies.

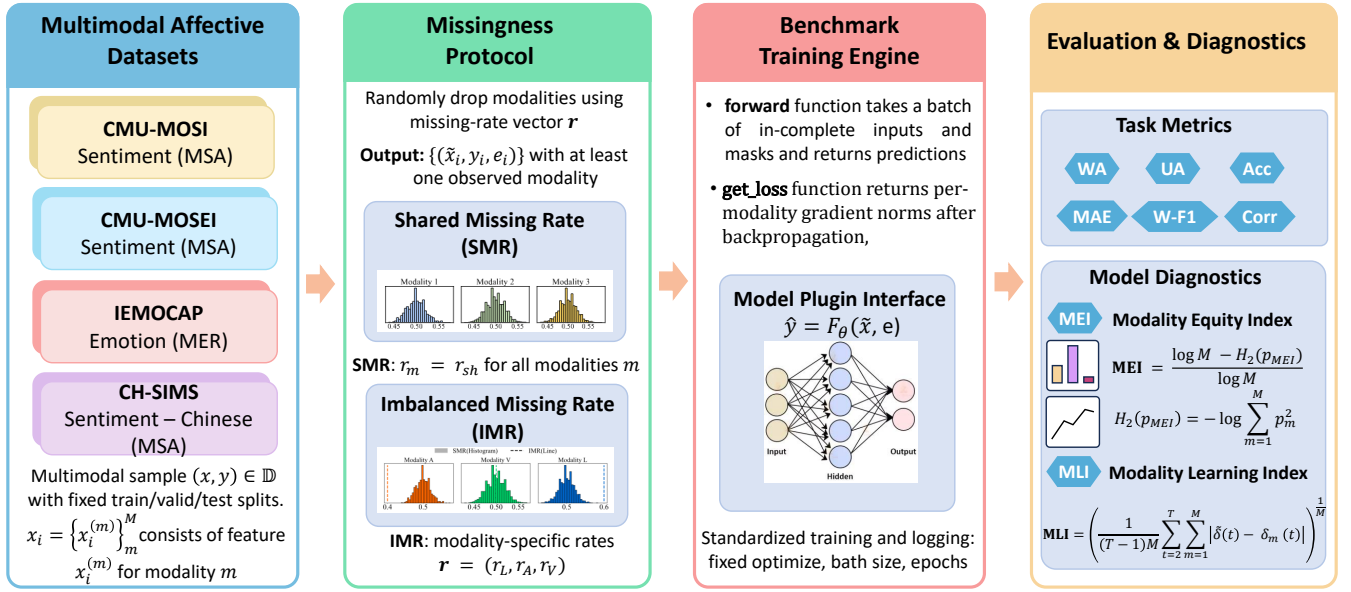


Figure 3: MissBench benchmark pipeline for multimodal affective tasks, illustrating data preparation, SMR/IMR missingness protocols, unified training with model plugins, and evaluation with both task metrics and modality-aware diagnostics.

Incomplete multimodal learning and missing modalities. A large body of methods has been proposed to address missing modalities. Representative approaches include imagination-based reconstruction, graph-based completion, and generative or robust architectures for incomplete multimodal inputs [10, 17, 27, 32, 40]. These methods significantly improve robustness compared to naive fusion. However, most of them assume fixed or shared missing patterns and are evaluated on a limited set of datasets. Evaluation is predominantly conducted using task-level metrics such as accuracy, F1-score, and MAE. In particular, the effect of systematically imbalanced missing rates on modality equity and learning dynamics is not explicitly analyzed.

Benchmarks and multimodal imbalance. Several benchmarks have been proposed to evaluate robustness in multimodal learning. MultiBench [12] and related efforts provide broad evaluations across tasks and domains [11, 26, 30]. These benchmarks mainly focus on balanced corruption or generic robustness scenarios. They do not explicitly distinguish shared and imbalanced missing-rate regimes. They also lack modality-aware diagnostic metrics beyond task performance. Recent work on multimodal imbalance and IMR-aware learning, such as BalanceBenchmark [31], RedCore [25], and MCE [38], studies unequal modality contributions and imbalanced missing rates. However, these efforts either target general multimodal tasks without affective-specific protocols or adopt method-specific setups that hinder direct comparison. MissMAC-Bench [15] introduces a benchmark for missing modality issues in multimodal affective computing. It evaluates holistic robustness under fixed and random missing patterns using competence-resilience measures. However, it does not explicitly model imbalanced missing rates or provide modality-level or optimization-level diagnostics.

As summarized in Table 1, existing methods and benchmarks leave a clear gap: none simultaneously standardizes shared and imbalanced missing-rate protocols for multimodal affective tasks while exposing both modality-level contributions and optimization dynamics. As a result, evaluations may report similar task accuracy while masking substantial differences in modality dominance and learning imbalance. MissBench is designed to fill this gap.

3 MissBench Design

Figure 3 summarizes the four phases of MissBench, including dataset organization, missingness protocol generation, standardized training, and modality-aware evaluation.

3.1 Datasets and Tasks

Datasets. Let $\mathbb{D} = \{(x_i, y_i)\}_{i=1}^N$ be a multimodal dataset with M modalities and label space \mathcal{Y} . Each input $x_i = \{x_i^{(m)}\}_{m=1}^M$ consists of features $x_i^{(m)} \in \mathbb{R}^{d_m}$ for modality m . MissBench adopts four affective datasets with three core modalities: language (L), visual (V), and acoustic (A), namely IEMOCAP [2], CMU-MOSI [34], CMU-MOSEI [35], and CH-SIMS [33].

After applying a masking protocol (Section 3.2), each clean input x_i is transformed into an incomplete sample $\tilde{x}_i = \{\tilde{x}_i^{(m)}\}_{m=1}^M$, forming the corrupted dataset $\tilde{\mathbb{D}} = \{(\tilde{x}_i, y_i)\}_{i=1}^N$. We always ensure that at least one modality remains observed in every sample so that supervision is well defined.

Task formulation. Given an incomplete sample \tilde{x}_i , a multimodal model F_θ produces a prediction $\hat{y}_i = F_\theta(\tilde{x}_i)$. MissBench considers two task families.

Multimodal Emotion Recognition (MER). On IEMOCAP, the label space is a set of emotion categories $\mathcal{Y}_{\text{MER}} = \{1, \dots, C\}$. The training

objective is multiclass classification with cross-entropy loss:

$$\mathcal{L}_{\text{MER}}(\theta) = \frac{1}{N} \sum_{i=1}^N \ell_{\text{CE}}(\hat{y}_i, y_i) \quad (1)$$

We report weighted accuracy (WA), unweighted accuracy (UA), and weighted F1-score (W-F1) as MER metrics.

Multimodal Sentiment Analysis (MSA). On CMU-MOSI, CMU-MOSEI, and CH-SIMS, each utterance is annotated with a real-valued sentiment intensity label. Let $y_i^{\text{reg}} \in \mathbb{R}$ denote the intensity label. The model outputs \hat{y}_i^{reg} , we use the following regression loss:

$$\mathcal{L}_{\text{MSA}}(\theta) = \frac{1}{N} \sum_{i=1}^N \ell_{\text{reg}}(\hat{y}_i^{\text{reg}}, y_i^{\text{reg}}) \quad (2)$$

where ℓ_{reg} is a regression loss (e.g., MAE or MSE). For evaluation, we follow common practice and report binary accuracy (Acc-2), weighted F1-score (WAF), mean absolute error (MAE), and Pearson correlation (Corr).

Throughout this paper, training under SMR and IMR corresponds to minimizing the same task loss (MER or MSA) with masks drawn from p_{SMR} and p_{IMR} , respectively. Section 3.3 introduces MEI and MLI to measure how these different masking distributions lead to inequity in modality contribution and optimization dynamics.

3.2 Missingness Protocol

Given a clean multimodal dataset \mathbb{D} , MissBench generates incomplete samples by applying a stochastic masking operator $\mathcal{M}(\cdot; \mathbf{r})$ parameterized by a missing-rate vector \mathbf{r} .

Masking operator. For each sample $x_i = \{x_i^{(m)}\}_{m=1}^M$ and missing-rate vector $\mathbf{r} = [r_1, \dots, r_M]$, the operator draws a binary mask $e_i = \{e_i^{(m)}\}_{m=1}^M$ with $e_i^{(m)} \in \{0, 1\}$, $\sum_m e_i^{(m)} \geq 1$. The incomplete sample $\tilde{x}_i^{(m)}$ is constructed as $\tilde{x}_i^{(m)} = x_i^{(m)}$ if $e_i^{(m)} = 1$, and $\vec{0}$ otherwise. MissBench instantiates two families of masking distributions, corresponding to shared and imbalanced missing-rate regimes.

Shared Missing Rate (SMR) Under SMR, all modalities share the same missing probability $r_{\text{sh}} \in [0, 1)$. Each modality m in sample i is independently retained with probability $1 - r_{\text{sh}}$ and dropped with probability r_{sh} :

$$\Pr(e_i^{(m)} = 1) = 1 - r_{\text{sh}}, \quad \Pr(e_i^{(m)} = 0) = r_{\text{sh}} \quad (3)$$

The induced distribution over a masking pattern $e = \{e^{(m)}\}_{m=1}^M$ is:

$$p_{\text{SMR}}(e) = \frac{\prod_{m=1}^M (1 - r_{\text{sh}})^{e^{(m)}} r_{\text{sh}}^{1-e^{(m)}}}{1 - r_{\text{sh}}^M} \quad (4)$$

where the denominator excludes the all-missing case. Under this regime, the empirical missing ratios $\hat{r}_m = \frac{1}{N} \sum_{i=1}^N (1 - e_i^{(m)})$ concentrate around r_{sh} as N grows, ensuring that all modalities are statistically symmetric and any observed differences arise from random fluctuation rather than systematic imbalance.

Imbalanced Missing Rate (IMR) In realistic scenarios, different modalities have heterogeneous missing probabilities $r_m \neq r_{m'}$. MissBench models this by assigning each modality its own missing ratio $r_m \in [0, 1)$ and defining:

$$p_{\text{IMR}}(e) = \frac{\prod_{m=1}^M (1 - r_m)^{e^{(m)}} r_m^{1-e^{(m)}}}{1 - \prod_{m=1}^M r_m} \quad (5)$$

Compared with a mean-matched SMR distribution, p_{IMR} concentrates probability mass on patterns that retain low- r_m modalities while dropping high- r_m ones, creating systematic exposure imbalance across modalities. The degree of imbalance can be quantified by a divergence: $\Delta_{\text{IMR}} = \mathcal{D}(p_{\text{IMR}}(e) \parallel p_{\text{SMR}}(e))$, where \mathcal{D} can be, for example, KL or Jensen–Shannon divergence. Larger Δ_{IMR} indicates stronger modality heterogeneity and a more biased sampling of multimodal patterns.

3.3 Metrics for Modality Equity and Optimization

Given a multimodal model F_θ trained under a masking protocol (SMR or IMR), MissBench evaluates not only task performance but also the equity of modality contributions and the balance of optimization dynamics. We formalize F_θ as consisting of \mathcal{M} modules $\{f_{\theta_1}, \dots, f_{\theta_M}\}$, where each module f_{θ_i} typically corresponds to a modality encoder or a shared fusion component. We introduce two diagnostic metrics: the *Modality Equity Index (MEI)* and the *Modality Learning Index (MLI)*.

3.3.1 Modality Equity Index (MEI). It measures how evenly different modalities contribute to predictive performance by evaluating model behavior across all possible missing-modality configurations.

To compute MEI, we evaluate the trained model on the uncorrupted test dataset \mathcal{S} under synthetic missing-modality patterns. For each modality m , let C_m denote the set of all modality combinations in which m is unavailable, with $|C_m| = 2^{M-1} - 1$. For a specific combination $\hat{c} \in C_m$, we construct a synthetic test set $\mathcal{S}_{\hat{c}}$ by replacing features of modalities not in \hat{c} with zero vectors $\vec{0}$. Let $\text{Perf}_{\hat{c}}$ be the task-specific performance score of F_θ on $\mathcal{S}_{\hat{c}}$.

We first measure the performance fluctuation associated with modality m across all combinations in C_m :

$$\mathbf{s}_m = \{\text{Perf}_{\text{full}} - \text{Perf}_{\hat{c}} : \hat{c} \in C_m\} \quad (6)$$

where $\mathbf{s}_m \in \mathbb{R}^{|C_m|}$ captures the performance drop when m is removed in each combination. The contribution of modality m is characterized by the mean $\mu_m = \mathbb{E}[\mathbf{s}_m]$ and standard deviation $\sigma_m = \sqrt{\text{Var}(\mathbf{s}_m)}$.

We then normalize the contribution as:

$$\zeta_m = \frac{\mu_m}{\sigma_m + \varepsilon} \quad (7)$$

where $\varepsilon > 0$ ensures numerical stability. This normalization yields a signal-to-noise ratio: modalities with consistent, large performance drops have high $|\zeta_m|$, while those with noisy or small drops have low $|\zeta_m|$.

To construct a probability distribution over modality contributions, we define:

$$p_m = \frac{|\zeta_m|}{\sum_{m'=1}^M |\zeta_{m'}| + \varepsilon}, \quad m = 1, \dots, M \quad (8)$$

and let $p_{\text{MEI}} = [p_1, p_2, \dots, p_M]$ represent the normalized contribution distribution. Here, we use the magnitude $|\zeta_m|$ to capture the strength of modality m 's contribution regardless of sign, as large absolute values indicate strong impact (beneficial if $\zeta_m > 0$, detrimental if $\zeta_m < 0$).

Finally, MEI is defined as:

$$\text{MEI} = \frac{\log M - H_2(\mathbf{p}_{\text{MEI}})}{\log M} \quad (9)$$

where $H_2(\mathbf{p}) = -\log \sum_{m=1}^M p_m^2$ is the Rényi entropy of order 2. MEI ranges from 0 (one modality dominates) to 1 (perfectly balanced contribution). High MEI indicates that all modalities contribute evenly, while low MEI signals that one or a few modalities dominate task performance.

3.3.2 Modality Learning Index (MLI). MLI quantifies optimization imbalance by comparing gradient magnitudes across modalities during training.

Let $\mathcal{L}^{(t)} = \frac{1}{N} \sum_{i=1}^N \ell_i^{(t)}$ be the task loss at iteration t . We define the *modality-specific loss* for modality m as the average loss over samples in which m is available:

$$\mathcal{L}_m^{(t)} = \frac{\sum_{i=1}^N e_i^{(m)} \ell_i^{(t)}}{\sum_{i=1}^N e_i^{(m)}} \quad (10)$$

where $e_i^{(m)} \in \{0, 1\}$ indicates whether modality m is observed in sample i . For each module f_{θ_k} , we compute its modality-specific gradient vector at step t via:

$$\mathbf{g}_{\theta_k}^m(t) = \frac{\partial \mathcal{L}_m^{(t)}}{\partial \theta_k} \quad (11)$$

The optimization magnitude for modality m is then estimated by averaging gradient norms across all M modules:

$$G_m(t) = \frac{1}{M} \sum_{k=1}^M \|\mathbf{g}_{\theta_k}^m(t)\|_2 \quad (12)$$

This aggregation provides a holistic view of how strongly modality m drives parameter updates across the entire model.

We define the temporal gradient variation of modality m at training step t as:

$$\delta_m(t) = |G_m(t) - G_m(t-1)|, \quad t = 2, \dots, T \quad (13)$$

which quantifies the change in the magnitude of the uni-modal gradient between consecutive iterations. T denotes the total number of training iterations, and $\delta_m(t)$ is defined from the second iteration onward. To capture the overall update behavior across modalities, we further compute the cross-modal variation:

$$\bar{\delta}(t) = \frac{1}{M} \sum_{m=1}^M \delta_m(t) \quad (14)$$

Finally, our metric MLI is formulated as:

$$\text{MLI} = \left(\frac{1}{\max_t \bar{\delta}(t)(T-1)M} \sum_{t=2}^T \sum_{m=1}^M |\bar{\delta}(t) - \delta_m(t)| \right)^{\frac{1}{M}} \quad (15)$$

Overall, MLI measures the extent to which individual modalities deviate from the shared update dynamics throughout training. $\text{MLI} \in [0, 1]$, where lower values indicate more consistent and balanced temporal updates across modalities, whilst higher values reflect heterogeneous update stability, suggesting asynchronous optimization during learning.

3.4 Benchmark Pipeline and Model Plugin

MissBench provides a unified pipeline that applies missingness protocols, trains models, and evaluates arbitrary methods through a simple plugin interface, ensuring fair comparison under identical masking, training, and evaluation conditions.

Overall pipeline. Given a clean dataset \mathbb{D} , MissBench first applies a chosen missingness protocol (SMR or IMR) to generate the corrupted dataset $\tilde{\mathbb{D}} = \{(\tilde{x}_i, y_i)\}_{i=1}^N$ together with binary masks e_i that indicate which modalities remain observed in each sample. During training, the benchmark repeatedly samples mini-batches $\{(\tilde{x}_i, e_i, y_i)\}$, feeds them to a user-specified model plugin F_θ , and optimizes the total objective. The pipeline supports flexible optimization by aggregating the task loss (MER or MSA) with any model-specific auxiliary losses returned by the plugin. At evaluation time, task metrics are computed on held-out data, and MEI and MLI are derived from logged performance and gradient statistics.

Model plugin interface. To integrate a new method, users implement a model plugin that exposes two functions: forward and get_loss. The forward function takes a batch of incomplete inputs and masks as input, and returns predictions and intermediate representations:

$$\hat{y}, z = F_\theta(\tilde{x}, e) \quad (16)$$

where z denotes optional auxiliary outputs and e allows the model to identify missing modalities without accessing ground-truth full features. The get_loss function then consumes these outputs to compute auxiliary objectives, allowing the benchmark to support complex multi-task learning frameworks. By offloading diagnostics to external MLI and MEI modules, we eliminate the need for complex internal hooks within the model.

Standardized training and logging. All methods are trained under the same optimization budget: identical batch size, optimizer, number of epochs, and early-stopping criterion. This ensures that differences in results arise from modeling choices rather than hyperparameter tuning advantages. During training, MissBench logs per-epoch task metrics, modality-wise performance on validation data, and uses the MLI evaluator to track the fluctuation of gradient norms for each modality. These logs enable the computation of MLI over the training trajectory. Complementing this, MEI is evaluated through a separate ablation inference loop on the valid and test set, and these metrics jointly provide a consistent diagnostic view of how each model behaves under SMR and IMR protocols.

4 MissBench Empirical Analysis

4.1 Experimental Setup

We evaluate MissBench on four multimodal affective datasets (IEMO-CAP [2], CMU-MOSI [34], CMU-MOSEI [35], CH-SIMS [33]) with language, acoustic, and visual modalities, following the standard MER/MSA protocols and official splits when available. Compared methods cover three families: (i) IMR-aware approaches (RedCore [25], MCE [38]), (ii) missing-modality handling models (MMIN [40], GCNet [10], SDR-GNN [6], Mi-CGA [19]), and (iii) gradient-based or generic baselines (Ada2I [20], OGM-GE [21], naive fusion).

We evaluate all methods under identical training budgets (optimizer, batch size, number of epochs) and report results for both SMR and IMR masking protocols with fixed random seeds to ensure

Table 2: MEI_{UA}/MLI(%) of representatives from each method-family.

Method	Setting	IEMOCAP						CMU-MOSI					
		0.3 / (0.1,0.2,0.6)		0.5 / (0.2,0.5,0.8)		0.7 / (0.4,0.8,0.9)		0.3 / (0.1,0.2,0.6)		0.5 / (0.2,0.5,0.8)		0.7 / (0.4,0.8,0.9)	
		MEI _{UA}	MLI	MEI _{UA}	MLI	MEI _{UA}	MLI	MEI _{UA}	MLI	MEI _{UA}	MLI	MEI _{UA}	MLI
GCNet	SMR	8.21 \pm 5.40	31.56 \pm 3.08	11.41 \pm 8.31	38.83 \pm 6.99	20.57 \pm 17.78	41.15 \pm 6.45	79.67 \pm 14.41	34.77 \pm 7.29	76.67 \pm 7.15	43.12 \pm 8.51	48.75 \pm 30.61	62.42 \pm 5.19
	IMR	7.33 \pm 2.48	32.89 \pm 3.55	30.71 \pm 34.82	42.52 \pm 8.69	25.06 \pm 28.70	41.97 \pm 4.62	70.83 \pm 10.94	41.06 \pm 9.81	71.24 \pm 18.21	55.85 \pm 10.38	79.90 \pm 15.55	58.02 \pm 9.19
RedCore	SMR	5.92 \pm 2.71	34.77 \pm 7.29	13.45 \pm 8.89	44.03 \pm 2.64	11.48 \pm 10.00	43.12 \pm 8.51	88.08 \pm 2.50	34.28 \pm 2.56	85.04 \pm 3.57	41.76 \pm 5.30	83.57 \pm 8.65	49.20 \pm 5.40
	IMR	7.06 \pm 1.73	41.06 \pm 9.81	8.39 \pm 10.67	46.81 \pm 4.34	5.63 \pm 2.50	55.85 \pm 10.38	86.85 \pm 2.03	40.39 \pm 5.54	87.16 \pm 2.13	40.86 \pm 7.70	80.58 \pm 6.82	51.01 \pm 2.50
Ada2I	SMR	10.65 \pm 6.85	32.87 \pm 1.71	6.77 \pm 7.77	38.00 \pm 3.35	10.21 \pm 8.54	39.50 \pm 5.47	67.60 \pm 18.78	32.87 \pm 2.79	60.40 \pm 17.71	38.85 \pm 3.91	42.91 \pm 22.21	39.50 \pm 5.13
	IMR	10.58 \pm 12.20	35.48 \pm 3.27	9.68 \pm 8.71	41.73 \pm 6.45	20.86 \pm 25.99	43.69 \pm 2.07	40.47 \pm 19.05	35.48 \pm 4.47	50.97 \pm 36.04	38.16 \pm 4.37	49.23 \pm 14.34	43.69 \pm 2.85

fair and reproducible comparisons. Our empirical study is organized around the following research questions:

RQ1 (Shared missing rates). Do existing methods behave as expected under standard shared missing rates (SMR), in terms of both task performance and modality/gradients diagnostics?

RQ2 (Mean-matched IMR). When the average missing rate remains constant, how does moving from SMR to imbalanced missing rates (IMR) affect performance, MEI, and MLI?

RQ3 (Extreme IMR and trade-offs). Under more extreme IMR scenarios, how do different method families trade off task accuracy against modality equity (MEI) and optimization balance (MLI)?

4.2 Behavior under Shared Missing Rates (SMR)

Task-level performance under SMR. We address **RQ1** by examining model behavior under shared missing rates (SMR). Figure 4 shows that, across all datasets, task performance degrades smoothly and monotonically as the shared missing ratio increases, confirming that SMR induces a controlled and predictable degradation. IMR-aware models and dedicated missing-modality handlers consistently outperform naive fusion and generic baselines, with more pronounced gains at moderate to high missing ratios (0.3–0.7).

However, similar task-level trends may arise from fundamentally different modality usage patterns, which cannot be distinguished by accuracy alone.

MEI and MLI under SMR. Table 2 reveals substantial dataset-dependent differences in modality equity and optimization balance under SMR. On IEMOCAP, all models exhibit low MEI_{UA} (mostly below 25) together with relatively high MLI values, indicating pronounced modality and optimization imbalance even under symmetric missing patterns. In contrast, on CMU-MOSI, the same models achieve much higher MEI_{UA} (typically 70–90) with more moderate MLI, suggesting more balanced modality exploitation.

Overall, while SMR provides a stable baseline with smooth task degradation, modality equity and learning balance vary substantially across datasets. Notably, IEMOCAP already exhibits strong imbalance under SMR, motivating the more challenging IMR settings examined next.

4.3 Mean-matched SMR vs IMR

Mean-matched protocol. To isolate the effect of imbalance from overall missing severity, we construct SMR–IMR pairs with matched expected missing ratios. Under SMR with rate r_{sh} , the expected number of missing modalities per sample is Mr_{sh} , whereas under IMR with modality-specific rates $\mathbf{r} = (r_1, \dots, r_M)$ it is $\sum_{m=1}^M r_m$. We

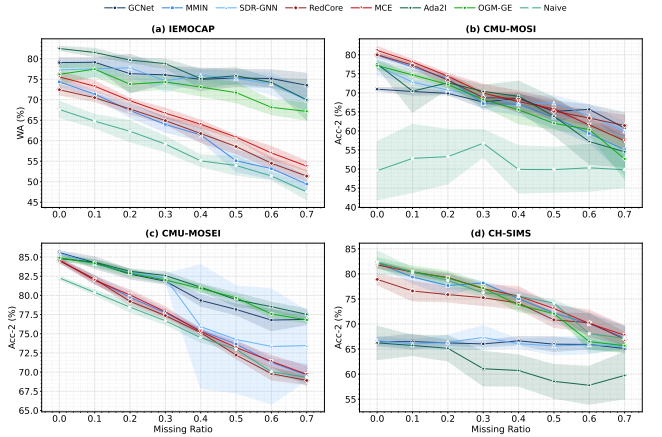


Figure 4: Performance of multimodal methods under shared missing rates (SMR) on IEMOCAP (WA) and CMU-MOSI/MOSEI/CH-SIMS (Acc-2). IMR-aware methods are shown in red, missing-modality handling models in blue, and gradient-based or generic baselines in green.

define the mean-matched condition as:

$$Mr_{sh} \approx \sum_{m=1}^M r_m. \quad (17)$$

Under this constraint, SMR and IMR exhibit comparable overall missingness, and observed differences can be attributed to imbalance in modality exposure rather than total missing data.

We instantiate three mean-matched pairs corresponding to *low*, *medium*, and *high* missing regimes with $r_{sh} \in \{0.3, 0.5, 0.7\}$. Each SMR setting is paired with an IMR configuration whose (r_A, r_V, r_L) values approximate the same average missing ratio. We assign higher missing rates to language to reflect its dominant role in many multimodal affective models; however, this choice is illustrative, and MissBench supports arbitrary SMR/IMR configurations and modality orderings.

Task performance under mean-matched SMR vs. IMR. On CMU-MOSI (Table 3), moving from SMR to mean-matched IMR consistently degrades task performance across all method families. For missing-modality handlers such as MMIN and GCNet, Acc-2 drops by approximately 3–10 points at the same mean missing level, accompanied by higher MAE and lower correlation across low, medium, and high regimes. IMR-aware methods also incur

Table 3: Task performance on CMU-MOSI under SMR and mean-matched IMR across low, medium, and high missing regimes. For IMR, modality-specific rates follow the order (r_A, r_V, r_L) .

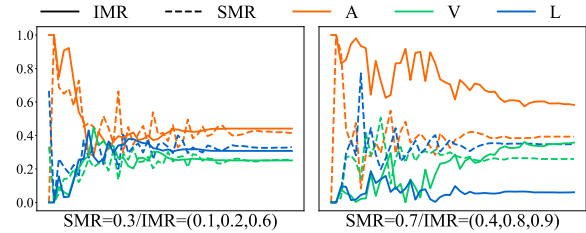
Method	Setting	0.3 / (0.1, 0.2, 0.6)			0.5 / (0.2, 0.5, 0.8)			0.7 / (0.4, 0.8, 0.9)		
		Acc-2(\uparrow)	MAE(\downarrow)	Corr(\uparrow)	Acc-2(\uparrow)	MAE(\downarrow)	Corr(\uparrow)	Acc-2(\uparrow)	MAE(\downarrow)	Corr(\uparrow)
MMIN	SMR	67.20 \pm 1.48	1.180 \pm 0.085	0.543 \pm 0.025	63.57 \pm 2.82	1.249 \pm 0.008	0.472 \pm 0.015	55.09 \pm 6.66	1.374 \pm 0.064	0.331 \pm 0.092
	IMR	61.80 \pm 1.43	1.288 \pm 0.017	0.425 \pm 0.020	55.61 \pm 3.86	1.398 \pm 0.042	0.305 \pm 0.064	52.59 \pm 4.11	1.425 \pm 0.027	0.293 \pm 0.027
GCNet	SMR	67.59 \pm 1.60	1.227 \pm 0.025	0.453 \pm 0.014	65.15 \pm 2.77	1.283 \pm 0.057	0.428 \pm 0.020	60.79 \pm 4.01	1.387 \pm 0.043	0.284 \pm 0.070
	IMR	64.33 \pm 3.04	1.316 \pm 0.055	0.346 \pm 0.073	55.58 \pm 3.78	1.436 \pm 0.043	0.167 \pm 0.066	55.95 \pm 4.01	1.425 \pm 0.058	0.208 \pm 0.043
RedCore	SMR	68.75 \pm 1.59	1.188 \pm 0.032	0.509 \pm 0.013	65.21 \pm 1.73	1.256 \pm 0.008	0.433 \pm 0.023	61.43 \pm 2.70	1.347 \pm 0.047	0.352 \pm 0.047
	IMR	62.87 \pm 2.14	1.307 \pm 0.029	0.393 \pm 0.033	59.48 \pm 2.09	1.372 \pm 0.022	0.323 \pm 0.029	54.60 \pm 5.43	1.424 \pm 0.038	0.258 \pm 0.117
MCE	SMR	69.97 \pm 2.29	1.146 \pm 0.041	0.547 \pm 0.015	65.79 \pm 2.60	1.230 \pm 0.028	0.467 \pm 0.015	57.44 \pm 2.06	1.357 \pm 0.037	0.367 \pm 0.037
	IMR	63.35 \pm 1.49	1.300 \pm 0.029	0.413 \pm 0.021	58.05 \pm 1.23	1.381 \pm 0.017	0.323 \pm 0.034	57.96 \pm 1.49	1.367 \pm 0.015	0.335 \pm 0.014
Ada2I	SMR	70.40 \pm 1.65	1.380 \pm 0.097	0.494 \pm 0.027	63.87 \pm 4.92	1.387 \pm 0.097	0.362 \pm 0.091	54.54 \pm 4.07	1.472 \pm 0.065	0.158 \pm 0.089
	IMR	57.47 \pm 3.24	1.494 \pm 0.106	0.234 \pm 0.093	55.12 \pm 2.87	1.452 \pm 0.042	0.174 \pm 0.071	52.10 \pm 3.94	1.552 \pm 0.080	0.134 \pm 0.072
OGM-GE	SMR	68.24 \pm 1.80	1.234 \pm 0.026	0.450 \pm 0.030	62.02 \pm 1.56	1.315 \pm 0.029	0.360 \pm 0.043	52.67 \pm 5.31	1.444 \pm 0.042	0.144 \pm 0.099
	IMR	59.76 \pm 3.13	1.375 \pm 0.050	0.278 \pm 0.073	53.38 \pm 2.73	1.453 \pm 0.031	0.138 \pm 0.077	51.98 \pm 3.65	1.468 \pm 0.036	0.119 \pm 0.052

Table 4: Task performance on IEMOCAP under SMR and mean-matched IMR across low, medium, and high missing regimes. IMR configurations are reported using the modality order (r_A, r_V, r_L) .

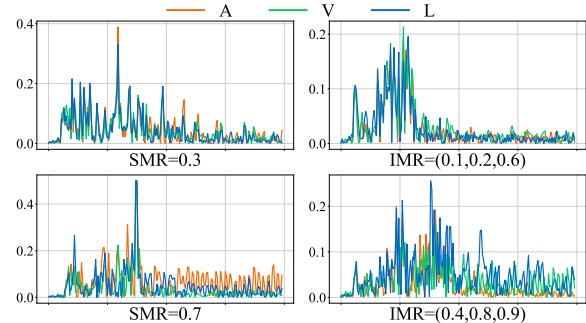
Method	Setting	0.3 / (0.1, 0.2, 0.6)		0.5 / (0.2, 0.5, 0.8)		0.7 / (0.4, 0.8, 0.9)	
		WA	F1	WA	F1	WA	F1
MMIN	SMR	63.98 \pm 1.90	64.30 \pm 1.88	55.10 \pm 2.60	55.36 \pm 2.67	49.43 \pm 1.96	49.51 \pm 1.94
	IMR	61.00 \pm 2.53	61.19 \pm 2.57	55.55 \pm 1.95	55.91 \pm 1.91	50.25 \pm 1.72	50.18 \pm 2.03
GCNet	SMR	76.07 \pm 2.06	76.23 \pm 1.95	75.33 \pm 2.04	75.49 \pm 1.99	73.52 \pm 2.95	73.54 \pm 2.89
	IMR	73.70 \pm 3.58	73.96 \pm 3.26	65.21 \pm 4.47	65.35 \pm 4.67	65.61 \pm 3.70	66.09 \pm 3.69
RedCore	SMR	64.90 \pm 0.88	65.15 \pm 0.92	58.58 \pm 1.69	58.82 \pm 1.66	51.36 \pm 1.30	51.71 \pm 1.28
	IMR	62.69 \pm 2.17	62.72 \pm 2.18	57.16 \pm 1.58	57.34 \pm 1.60	52.38 \pm 1.09	52.53 \pm 1.01
MCE	SMR	66.72 \pm 1.20	66.93 \pm 1.18	60.87 \pm 0.44	61.06 \pm 0.47	53.80 \pm 1.19	53.97 \pm 1.16
	IMR	63.87 \pm 1.16	63.98 \pm 1.16	59.27 \pm 1.03	59.48 \pm 0.96	54.44 \pm 1.38	54.47 \pm 1.37
Ada2I	SMR	78.81 \pm 1.10	78.81 \pm 1.22	75.86 \pm 1.95	76.00 \pm 1.89	69.99 \pm 4.92	70.26 \pm 5.11
	IMR	76.52 \pm 2.39	76.67 \pm 2.31	71.97 \pm 2.14	72.34 \pm 2.18	71.94 \pm 2.22	72.40 \pm 2.21
OGM-GE	SMR	74.34 \pm 1.76	74.62 \pm 1.67	71.74 \pm 2.47	71.85 \pm 2.25	67.16 \pm 2.14	67.24 \pm 2.11
	IMR	70.93 \pm 3.15	71.11 \pm 3.21	63.35 \pm 3.89	63.51 \pm 3.80	63.05 \pm 1.62	63.72 \pm 1.52

non-trivial losses. For example, RedCore’s Acc-2 decreases from 68.8 to 62.9 in the low regime and from 61.4 to 54.6 in the high regime, with corresponding increases in MAE and decreases in Corr. Generic or gradient-based baselines are the most sensitive. Ada2I’s Acc-2 drops from 70.4 to 57.5 under the low setting, and its correlation nearly halves from 0.494 to 0.234, with further degradation at higher missing levels.

On IEMOCAP (Table 4), a similar pattern is observed, though with greater variation across methods. GCNet and OGM-GE show substantial WA drops when switching from SMR to IMR, particularly at medium and high missing levels. For instance, GCNet decreases from 75.3 to 65.2 at the medium setting and from 73.5 to 65.6 at the high setting. IMR-aware methods such as RedCore and MCE exhibit smaller but consistent degradations at low and medium levels, with partial stabilization at the highest missing ratio. Ada2I experiences relatively mild WA degradation and even a slight improvement at the highest setting (from 70.0 to 71.9), but its absolute



(a) Modality contribution p_{MEI} on validation data (by epoch)



(b) Unimodal temporal gradient variation $\delta_m(t)$ from MLI (by step)

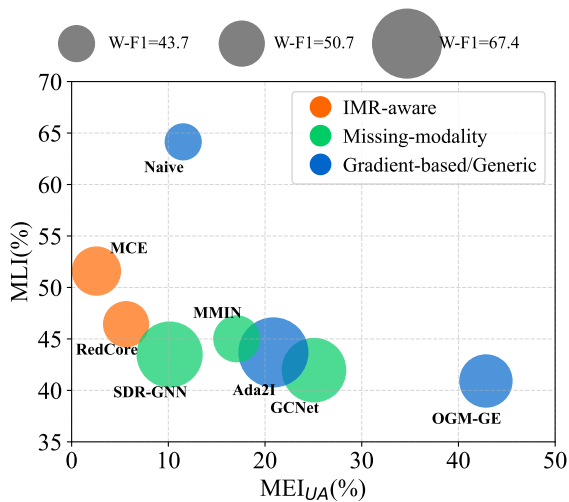
Figure 5: Statistics of GCNet [10] during training on IEMOCAP under different missing configurations.

performance remains below that of leading missing-modality handlers, and its instability on CMU-MOSI indicates limited robustness across tasks.

Bimodal analysis under mean-matched IMR. Table 5 reports bimodal results under mean-matched SMR and IMR settings. Across all modality pairs, moving from SMR to IMR consistently increases MLI and amplifies modality imbalance, even when task-level performance changes are modest. This effect is particularly evident in settings with reduced redundancy. For example, in the AV configuration, GCNet’s MEI_{UA} rises sharply under IMR at higher missing

Table 5: Performance comparison under different bimodal combinations (A: Audio, V: Visual, L: Language) and missing-rate settings, including Shared Missing Rate (SMR) and Imbalanced Missing Rate (IMR).

Method	Setting (AV)	0.1 / (0.1, 0.1)				0.3 / (0.1, 0.5)				0.5 / (0.6, 0.4)			
		WA	F1	MEI _{UA}	MLI	WA	F1	MEI _{UA}	MLI	WA	F1	MEI _{UA}	MLI
GCNet	SMR	68.07 \pm 3.55	68.57 \pm 3.43	38.45 \pm 16.94	13.20 \pm 3.21	64.88 \pm 3.01	65.17 \pm 3.30	52.18 \pm 34.67	15.87 \pm 4.57	64.56 \pm 3.08	65.11 \pm 2.70	41.05 \pm 32.08	18.19 \pm 5.21
	IMR	68.99 \pm 3.54	69.35 \pm 3.47	32.71 \pm 14.74	11.27 \pm 3.69	66.24 \pm 1.79	66.69 \pm 1.56	64.24 \pm 19.16	12.15 \pm 3.38	65.00 \pm 3.53	65.41 \pm 3.27	77.01 \pm 9.12	16.99 \pm 4.04
RedCore	SMR	60.35 \pm 1.47	60.60 \pm 1.32	10.42 \pm 6.40	15.73 \pm 1.34	54.68 \pm 0.73	54.79 \pm 0.74	3.60 \pm 4.78	22.50 \pm 1.53	48.62 \pm 2.04	47.33 \pm 3.74	2.77 \pm 3.59	28.95 \pm 3.57
	IMR	58.03 \pm 2.02	58.32 \pm 1.91	5.24 \pm 5.12	14.86 \pm 2.40	54.18 \pm 1.13	54.22 \pm 1.29	9.78 \pm 9.00	22.03 \pm 2.13	48.88 \pm 1.66	48.07 \pm 2.54	15.30 \pm 9.15	26.20 \pm 1.34
Ada2I	SMR	72.07 \pm 1.00	72.01 \pm 1.08	17.45 \pm 1.54	19.69 \pm 4.27	71.39 \pm 1.39	71.44 \pm 1.41	17.05 \pm 4.25	27.07 \pm 5.26	71.75 \pm 1.84	71.78 \pm 1.77	22.02 \pm 7.26	32.42 \pm 6.46
	IMR	71.80 \pm 1.21	71.65 \pm 1.45	19.08 \pm 3.66	16.95 \pm 3.35	72.38 \pm 0.58	72.56 \pm 0.48	20.76 \pm 1.77	23.88 \pm 3.96	67.83 \pm 3.23	67.89 \pm 3.19	14.69 \pm 7.76	24.53 \pm 2.70
Method	Setting (AL)	0.1 / (0.1, 0.1)				0.3 / (0.4, 0.2)				0.5 / (0.3, 0.7)			
		WA	F1	MEI _{UA}	MLI	WA	F1	MEI _{UA}	MLI	WA	F1	MEI _{UA}	MLI
GCNet	SMR	73.44 \pm 2.82	73.83 \pm 2.58	11.24 \pm 6.63	11.31 \pm 1.23	70.09 \pm 8.31	70.06 \pm 8.87	24.74 \pm 9.21	16.15 \pm 2.44	73.55 \pm 1.04	73.71 \pm 1.02	40.32 \pm 30.70	18.23 \pm 3.06
	IMR	75.34 \pm 2.28	75.51 \pm 2.25	9.51 \pm 6.44	13.22 \pm 3.37	73.84 \pm 5.17	73.97 \pm 4.88	25.97 \pm 20.36	18.00 \pm 1.37	66.48 \pm 8.18	65.68 \pm 10.43	20.88 \pm 22.84	18.13 \pm 5.53
RedCore	SMR	62.35 \pm 1.50	62.37 \pm 1.55	68.35 \pm 17.09	15.12 \pm 2.22	56.86 \pm 0.71	56.76 \pm 0.77	66.52 \pm 11.27	20.85 \pm 2.38	48.99 \pm 4.45	48.41 \pm 5.02	53.33 \pm 37.97	23.37 \pm 4.38
	IMR	62.71 \pm 0.71	62.75 \pm 0.69	60.44 \pm 13.37	14.76 \pm 2.15	58.63 \pm 2.55	58.46 \pm 2.81	61.94 \pm 13.93	20.40 \pm 3.49	46.58 \pm 2.85	44.85 \pm 3.76	60.46 \pm 19.69	24.21 \pm 1.79
Ada2I	SMR	79.85 \pm 1.37	80.08 \pm 1.32	6.78 \pm 5.18	13.94 \pm 1.75	75.95 \pm 3.15	76.15 \pm 3.18	7.98 \pm 6.37	18.13 \pm 1.79	75.21 \pm 0.71	75.41 \pm 0.59	12.41 \pm 6.55	25.63 \pm 4.16
	IMR	79.05 \pm 2.07	79.31 \pm 1.97	8.75 \pm 6.92	13.17 \pm 1.79	75.62 \pm 5.14	75.83 \pm 5.17	5.09 \pm 3.85	20.02 \pm 2.65	73.02 \pm 5.95	73.24 \pm 5.96	6.58 \pm 4.48	28.12 \pm 4.95
Method	Setting (VL)	0.1 / (0.1, 0.1)				0.3 / (0.1, 0.5)				0.5 / (0.2, 0.8)			
		WA	F1	MEI _{UA}	MLI	WA	F1	MEI _{UA}	MLI	WA	F1	MEI _{UA}	MLI
GCNet	SMR	77.82 \pm 0.81	77.75 \pm 0.75	43.86 \pm 19.16	11.00 \pm 1.87	77.94 \pm 1.61	77.86 \pm 1.53	75.00 \pm 17.23	17.20 \pm 3.21	75.04 \pm 2.19	74.77 \pm 2.08	80.74 \pm 12.41	20.08 \pm 2.67
	IMR	77.97 \pm 1.37	77.75 \pm 1.59	61.14 \pm 23.80	13.20 \pm 1.88	72.51 \pm 5.51	71.68 \pm 5.68	43.98 \pm 26.49	14.96 \pm 2.87	67.69 \pm 4.01	67.10 \pm 4.02	53.37 \pm 31.76	23.54 \pm 4.26
RedCore	SMR	65.62 \pm 0.53	65.70 \pm 0.98	51.91 \pm 11.02	13.80 \pm 1.23	57.50 \pm 1.91	56.75 \pm 2.63	36.30 \pm 14.96	22.57 \pm 3.48	53.36 \pm 1.89	52.69 \pm 2.06	41.69 \pm 13.55	29.94 \pm 2.66
	IMR	65.62 \pm 1.22	65.64 \pm 1.32	43.47 \pm 17.53	13.85 \pm 1.49	57.37 \pm 1.24	57.16 \pm 1.14	42.26 \pm 23.39	23.48 \pm 2.42	50.07 \pm 0.94	47.05 \pm 3.15	23.98 \pm 12.20	29.57 \pm 3.66
Ada2I	SMR	77.55 \pm 2.75	77.39 \pm 2.83	28.55 \pm 14.56	12.85 \pm 1.46	76.36 \pm 2.15	76.21 \pm 2.23	40.57 \pm 28.42	19.88 \pm 2.47	73.30 \pm 1.04	73.18 \pm 1.12	39.72 \pm 11.41	22.49 \pm 3.72
	IMR	77.76 \pm 2.56	77.60 \pm 2.70	42.70 \pm 32.25	14.30 \pm 1.75	73.60 \pm 3.18	73.35 \pm 3.37	30.68 \pm 16.59	20.03 \pm 3.31	68.36 \pm 4.29	67.80 \pm 4.36	13.87 \pm 13.41	22.94 \pm 4.32

**Figure 6: Performance of baselines on IEMOCAP under extreme IMR=(0.4,0.8,0.9).**

levels (e.g., from 41.05 to 77.01 at 0.5), indicating strong dominance of the less-missing modality alongside elevated MLI.

MEI and MLI under mean-matched settings. Building on the SMR analysis, we examine how modality equity and learning dynamics change under mean-matched IMR (RQ2). Across datasets, IMR consistently worsens modality-level behavior compared to SMR at the same mean missing level. On IEMOCAP, all representative

methods (GCNet, RedCore, and Ada2I) exhibit markedly higher MLI under IMR. For example, RedCore’s MLI increases from 34.8 to 43.1 under SMR and from 41.1 to 55.9 under IMR when moving from low to high missing regimes (Table 2). On CMU-MOSI, GCNet and RedCore retain relatively high MEI_{UA} under IMR, yet their MLI still rises substantially, while Ada2I shows unstable MEI_{UA} together with steadily increasing MLI, indicating compounded imbalance in both contribution and optimization.

Figure 5 provides a mechanistic illustration of these effects using GCNet on IEMOCAP. Under SMR, modality contribution trajectories remain stable across epochs, whereas IMR induces pronounced shifts during training, with modalities experiencing lower missing rates becoming increasingly dominant. This behavior is accompanied by higher temporal gradient volatility and reduced cross-modality similarity, explaining the elevated MLI values observed under IMR. Consistent trends are also observed in the bimodal setting (Table 5), where reduced modality redundancy further amplifies IMR-induced imbalance.

4.4 Beyond Mean-matched: Extreme IMR and Method Trade-offs

To address RQ3, we move beyond mean-matched settings and examine model behavior under an extreme IMR configuration (r_A, r_V, r_L) = (0.4, 0.8, 0.9).

Extreme IMR exposes distinct equity–stability trade-offs. Under this setting, different method families occupy clearly separated regions in the MEI–MLI plane on IEMOCAP (Figure 6). IMR-aware methods achieve relatively high MEI but incur noticeably higher MLI, while

missing-modality handling models cluster in an intermediate region. Gradient-based or generic baselines exhibit divergent behaviors, either reducing MLI at the expense of low MEI or maintaining moderate equity without competitive performance.

Training-time diagnostics reveal language-locking. Training-time analysis on IEMOCAP and CMU-MOSI shows that moving from SMR to IMR progressively shifts contribution trajectories toward the language modality. For GCNet (Figure 5), language dominates p_{MEI} and exhibits the largest temporal gradient variation, even when its missing rate is only moderately lower than the others. Similar trends are observed for RedCore and Ada2I across both datasets (Figures 10-11, reported in Appendix). These patterns indicate a *language-locking* failure mode under severe imbalance.

Failure modes beyond mean-matched IMR. Combined with the mean-matched results and the IMR sweep results reported in Tables 9-10 and Figure 8 (Appendix), extreme IMR reveals a distinct trade-off that does not surface under milder imbalance. Methods that appear well-behaved under SMR or mean-matched IMR can shift to markedly different regions of the MEI-MLI plane as imbalance intensifies or the dominant modality changes. These observations answer **RQ3** by exposing failure modes, such as language locking and severe gradient dominance, that remain invisible to task-level evaluation under symmetric missing rates.

5 Conclusion

We presented MissBench, a benchmark and framework for multimodal affective computing that standardizes shared and imbalanced missing-rate protocols on four popular datasets. By introducing the Modality Equity Index (MEI) and Modality Learning Index (MLI), MissBench complements accuracy-based evaluation with modality- and optimization-level diagnostics. Our experiments show that models can look robust under shared missing rates yet still suffer from modality inequity and gradient dominance under imbalanced conditions, even at matched mean missing ratios. MissBench thus offers a practical tool for stress-testing multimodal affective models in realistic incomplete-modality settings and motivates future methods that jointly optimize task performance, modality equity, and balanced learning dynamics.

References

- [1] Tadas Baltrusaitis, Amir Zadeh, Yao Chong Lim, and Louis-Philippe Morency. 2018. OpenFace 2.0: Facial Behavior Analysis Toolkit. In *2018 13th IEEE International Conference on Automatic Face & Gesture Recognition (FG 2018)*. IEEE Press, 59–66.
- [2] Carlos Busso, Murtaza Bulut, Chi-Chun Lee, Abe Kazemzadeh, Emily Mower, Samuel Kim, Jeannette N Chang, Sungbok Lee, and Shrikanth S Narayanan. 2008. IEMOCAP: Interactive emotional dyadic motion capture database. *Language resources and evaluation* 42 (2008), 335–359.
- [3] Gilles Degottex, John Kane, Thomas Drugman, Tuomo Raitio, and Stefan Scherer. 2014. COVAREP: A Collaborative Voice Analysis Repository for Speech Technologies. *ICASSP*.
- [4] Jacob Devlin, Ming-Wei Chang, Kenton Lee, and Kristina Toutanova. 2019. BERT: Pre-training of Deep Bidirectional Transformers for Language Understanding. In *Proceedings of the 2019 Conference of the North American Chapter of the Association for Computational Linguistics: Human Language Technologies, Volume 1 (Long and Short Papers)*. Association for Computational Linguistics, 4171–4186.
- [5] Florian Eyben, Martin Wöllmer, and Björn Schuller. 2010. Opensmile: the munich versatile and fast open-source audio feature extractor. In *Proceedings of the 18th ACM International Conference on Multimedia (MM '10)*. 1459–1462.
- [6] Fangze Fu, Wei Ai, Fan Yang, Yuntao Shou, Tao Meng, and Keqin Li. 2024. SDR-GNN: Spectral Domain Reconstruction Graph Neural Network for incomplete multimodal learning in conversational emotion recognition. *Knowledge-Based Systems* (2024), 112825.
- [7] Guimin Hu, Yi Xin, Weimin Lyu, Haojian Huang, Chang Sun, Zhihong Zhu, Lin Gui, Ruihu Cai, Erik Cambria, and Hasti Seifi. 2024. Recent trends of multimodal affective computing: A survey from NLP perspective. *arXiv preprint arXiv:2409.07388* (2024).
- [8] Gao Huang, Zhuang Liu, Laurens Van Der Maaten, and Kilian Q Weinberger. 2017. Densely connected convolutional networks. In *Proceedings of the IEEE conference on computer vision and pattern recognition*. 4700–4708.
- [9] iMotions. 2017. Facial Expression Analysis. <https://imotions.com/products/imotions-lab/modules/fea-facial-expression-analysis/>. Accessed: 2017.
- [10] Zheng Lian, Lan Chen, Licai Sun, Bin Liu, and Jianhua Tao. 2023. GCNet: Graph Completion Network for Incomplete Multimodal Learning in Conversation. *IEEE Transactions on Pattern Analysis and Machine Intelligence* (2023).
- [11] Zheng Lian, Licai Sun, Yong Ren, Hao Gu, Haiyang Sun, Lan Chen, Bin Liu, and Jianhua Tao. 2026. Merbench: A unified evaluation benchmark for multimodal emotion recognition. *IEEE Transactions on Pattern Analysis and Machine Intelligence* (2026).
- [12] Paul Pu Liang, Yiwei Lyu, Xiang Fan, Zetian Wu, Yun Cheng, Jason Wu, Leslie Chen, Peter Wu, Michelle A Lee, Yuke Zhu, et al. 2021. Multibench: Multi-scale benchmarks for multimodal representation learning. *Advances in neural information processing systems* 2021, DB1 (2021), 1.
- [13] Paul Pu Liang, Amir Zadeh, and Louis-Philippe Morency. 2024. Foundations & trends in multimodal machine learning: Principles, challenges, and open questions. *Comput. Surveys* 56, 10 (2024), 1–42.
- [14] Ronghao Lin and Haifeng Hu. 2024. Adapt and explore: Multimodal mixup for representation learning. *Information Fusion* 105 (2024), 102216.
- [15] Ronghao Lin, Honghao Lu, Ruixing Wu, Aolin Xiong, Qingong Chu, Qiaolin He, Sijie Mai, and Haifeng Hu. 2026. MissMAC-Bench: Building Solid Benchmark for Missing Modality Issue in Robust Multimodal Affective Computing. *arXiv preprint arXiv:2602.00811* (2026).
- [16] Mengmeng Ma, Jian Ren, Long Zhao, Davide Testuggine, and Xi Peng. 2022. Are multimodal transformers robust to missing modality?. In *Proceedings of the IEEE/CVF conference on computer vision and pattern recognition*. 18177–18186.
- [17] Mengmeng Ma, Jian Ren, Long Zhao, Sergey Tulyakov, Cathy Wu, and Xi Peng. 2021. Smil: Multimodal learning with severely missing modality. In *Proceedings of the AAAI Conference on Artificial Intelligence*, Vol. 35. 2302–2310.
- [18] Brian McFee, Colin Raffel, Dawen Liang, Daniel Ellis, Matt Mcvicar, Eric Battenberg, and Oriol Nieto. 2015. librosa: Audio and Music Signal Analysis in Python. 18–24.
- [19] Cam-Van Thi Nguyen, Hai-Dang Kieu, Quang-Thuy Ha, Xuan-Hieu Phan, and Duc-Trong Le. 2025. Mi-CGA: Cross-modal Graph Attention Network for robust emotion recognition in the presence of incomplete modalities. *Neurocomputing* 623 (2025), 129342. doi:10.1016/j.neucom.2025.129342
- [20] Cam-Van Thi Nguyen, The-Son Le, Anh-Tuan Mai, and Duc-Trong Le. 2024. Ada2I: Enhancing Modality Balance for Multimodal Conversational Emotion Recognition. In *Proceedings of the 32nd ACM International Conference on Multimedia*. 9330–9339.
- [21] Xiaokang Peng, Yake Wei, Andong Deng, Dong Wang, and Di Hu. 2022. Balanced multimodal learning via on-the-fly gradient modulation. In *Proceedings of the IEEE/CVF conference on computer vision and pattern recognition*. 8238–8247.
- [22] Soujanya Poria, Erik Cambria, Rajiv Bajpai, and Amir Hussain. 2017. A review of affective computing: From unimodal analysis to multimodal fusion. *Information fusion* 37 (2017), 98–125.
- [23] Md Kaykobad Reza, Ashley Prater-Bennette, and M Salman Asif. 2024. Robust multimodal learning with missing modalities via parameter-efficient adaptation. *IEEE Transactions on Pattern Analysis and Machine Intelligence* (2024).
- [24] Junjie Shi, Caozhi Shang, Zhaobin Sun, Li Yu, Xin Yang, and Zengqiang Yan. 2024. Passion: Towards effective incomplete multi-modal medical image segmentation with imbalanced missing rates. In *Proceedings of the 32nd ACM International Conference on Multimedia*. 456–465.
- [25] Jun Sun, Xinxin Zhang, Shoukang Han, Yu-Ping Ruan, and Taihao Li. 2024. RedCore: Relative advantage aware cross-modal representation learning for missing modalities with imbalanced missing rates. In *Proceedings of the AAAI Conference on Artificial Intelligence*, Vol. 38. 15173–15182.
- [26] Chengye Wang, Yuyuan Li, XiaoHua Feng, Chaochao Chen, Xiaolin Zheng, and Jianwei Yin. 2025. UMU-Bench: Closing the Modality Gap in Multimodal Unlearning Evaluation. In *The Thirty-ninth Annual Conference on Neural Information Processing Systems Datasets and Benchmarks Track*.
- [27] Yuanzhi Wang, Yong Li, and Zhen Cui. 2023. Incomplete multimodality-diffused emotion recognition. *Advances in Neural Information Processing Systems* 36 (2023), 17117–17128.
- [28] Yunxiao Wang, Meng Liu, Zhe Li, Yupeng Hu, Xin Luo, and Liqiang Nie. 2023. Unlocking the power of multimodal learning for emotion recognition in conversation. In *Proceedings of the 31st ACM International Conference on Multimedia*. 5947–5955.
- [29] Nan Wu, Stanislaw Jastrzebski, Kyunghyun Cho, and Krzysztof J Geras. 2022. Characterizing and overcoming the greedy nature of learning in multi-modal deep neural networks. In *International Conference on Machine Learning*. PMLR,

- 24043–24055.
- [30] Renjie Wu, Hu Wang, Hsiang-Ting Chen, and Gustavo Carneiro. 2024. Deep multimodal learning with missing modality: A survey. *arXiv preprint arXiv:2409.07825* (2024).
- [31] Shaoxuan Xu, Menglu Cui, Chengxiang Huang, Hongfa Wang, and Di Hu. 2025. Balance benchmark: A survey for multimodal imbalance learning. *arXiv preprint arXiv:2502.10816* (2025).
- [32] Wenxin Xu, Hexin Jiang, et al. 2024. Leveraging Knowledge of Modality Experts for Incomplete Multimodal Learning. In *ACM Multimedia 2024*.
- [33] Wenmeng Yu, Hua Xu, Fanyang Meng, Yilin Zhu, Yixiao Ma, Jiele Wu, Jiyun Zou, and Kaicheng Yang. 2020. Ch-sims: A chinese multimodal sentiment analysis dataset with fine-grained annotation of modality. In *Proceedings of the 58th annual meeting of the association for computational linguistics*. 3718–3727.
- [34] Amir Zadeh, Rowan Zellers, Eli Pincus, and Louis-Philippe Morency. 2016. Multimodal Sentiment Intensity Analysis in Videos: Facial Gestures and Verbal Messages. *IEEE Intelligent Systems* 31 (11 2016), 82–88.
- [35] AmirAli Bagher Zadeh, Paul Pu Liang, Soujanya Poria, Erik Cambria, and Louis-Philippe Morency. 2018. Multimodal language analysis in the wild: Cmu-mosei dataset and interpretable dynamic fusion graph. In *Proceedings of the 56th Annual Meeting of the Association for Computational Linguistics (Volume 1: Long Papers)*. 2236–2246.
- [36] Kaipeng Zhang, Zhanpeng Zhang, Zhifeng Li, and Yu Qiao. 2016. Joint face detection and alignment using multitask cascaded convolutional networks. *IEEE signal processing letters* 23, 10 (2016), 1499–1503.
- [37] Qingyang Zhang, Yake Wei, Zongbo Han, Huazhu Fu, Xi Peng, Cheng Deng, Qinghua Hu, Cai Xu, Jie Wen, Di Hu, et al. 2024. Multimodal fusion on low-quality data: A comprehensive survey. *arXiv preprint arXiv:2404.18947* (2024).
- [38] Binyu Zhao, Wei Zhang, and Zhaonian Zou. 2025. MCE: Towards a General Framework for Handling Missing Modalities under Imbalanced Missing Rates. *Pattern Recognition* (2025), 112591.
- [39] Fei Zhao, Chengcui Zhang, and Baocheng Geng. 2024. Deep multimodal data fusion. *ACM computing surveys* 56, 9 (2024), 1–36.
- [40] Jinming Zhao, Ruichen Li, and Qin Jin. 2021. Missing modality imagination network for emotion recognition with uncertain missing modalities. In *Proceedings of the 59th Annual Meeting of the Association for Computational Linguistics*. 2608–2618.

Appendices

A Benchmark Datasets

This section provides an overview of the benchmark datasets used in our experiments. We summarize their key characteristics, including modality composition, task settings, and data statistics, to support reproducibility and facilitate interpretation of the experimental results reported in the main paper.

Table 6: Statistical overview of the MER and MSA datasets.

Dataset	Dialogues			Utterances		
	train	valid	test	train	valid	test
IEMOCAP	120		31	5810		1623
CMU-MOSI	52	10	31	1284	229	686
CMU-MOSEI	2249	300	676	16326	1871	4659
CH-SIMS	60	59	59	1,368	456	457

IEMOCAP [2] is a dataset of two-person interactions where actors take part in scripted and improvised conversations to express different emotions. It contains five sessions, each divided into several utterances with categorical emotion labels. Following previous work, we use the common four-class emotion setting. Since the dataset only includes training and test sets, we further split the training data into training and validation sets with a ratio of r (default 0.1).

CMU-MOSI [34] & **CMU-MOSEI** [35] consist of monologue and movie review video clips annotated with sentiment intensity scores between -3 and 3 . Aligning with the sentiment analysis setting, the datasets are trained as a regression task and evaluated using binary sentiment classification by thresholding the scores at zero, where samples with scores below 0 are labeled as negative and those above 0 as positive. The official data splits are adopted in all experiments.

CH-SIMS [33] is a Chinese benchmark dataset designed for multimodal sentiment analysis. In contrast to the two datasets mentioned earlier, it offers both multimodal and unimodal sentiment labels, however, we make use of only the multimodal ones. The dataset contains over 2000 utterance-level video clips spanning a wide range of content such as films, television dramas, and variety programs. Each sample is manually labeled with a continuous sentiment score ranging from -1 (strongly negative) to 1 (strongly positive).

B Multimodal Feature Extraction

For the **IEMOCAP** dataset, we adopt the feature extraction procedures described in [40] to obtain feature representations for each modality. Specifically, acoustic features are extracted using the openSMILE toolkit [5], resulting in 130-dimensional frame-level feature vectors. For the visual modality, we use a pretrained DenseNet [8] and extract 342-dimensional sequential representations from video frames. Finally, we employ a pretrained BERT-large model [4] to derive 1024-dimensional contextual word embeddings for the textual features.

For the **CMU-MOSI** and **CMU-MOSEI** datasets, we encode the textual modality with a pretrained BERT model [4] and generate 768-dimensional contextual word embeddings. For the visual part,

we process each video frame with the Facet toolkit [9] and capture 35 facial action unit features. Finally, we extract acoustic features via the COVAREP toolkit [3] and obtain 74-dimensional feature vectors.

For the **CH-SIMS** dataset, we use a pre-trained Chinese BERT-base [4] model to obtain 768-dimensional word vectors. For the visual modality, we employ the MTCNN [36] algorithm together with the OpenFace2.0 toolkit [1] to perform face alignment and extract 709-dimensional frame-level features. Finally, we utilize the LibROSA [18] toolkit and extract 33-dimensional acoustic features, including log F0, MFCCs, and CQT.

C Baseline Methods

We categorize baseline methods into three groups according to how they address missing or imbalanced modalities. This organization clarifies their design assumptions and facilitates a structured comparison under SMR and IMR settings.

Missing Modality Handling Methods. This category includes methods explicitly designed to operate when one or more modalities are missing at inference time. These approaches typically rely on modality reconstruction, adaptive fusion, or robustness-oriented architectures to mitigate performance degradation caused by incomplete inputs.

MMIN [40] adopts a masking-based training strategy that randomly drops modalities and learns modality-invariant representations, so that the model can maintain performance when certain modalities are absent at test time.

GCNet [10] captures speaker and temporal dependencies with graph neural networks to handle incomplete conversations, and adopts a dual-task framework that jointly predicts target labels and reconstructs missing features to enhance robustness to modality absence.

SDR-GNN [6] integrates spectral analysis into a hypergraph framework to impute missing data while explicitly retaining high-frequency signals that are typically attenuated in conventional GNNs, thereby improving robustness under incomplete multimodal observations.

IMR-aware Methods. IMR-aware methods explicitly account for imbalanced modality exposure during training. Instead of assuming uniform or random missing patterns, they introduce mechanisms to promote modality equity under asymmetric missing rates.

RedCore [25] employs variational encoders to construct robust cross-modal representations and dynamically regulates auxiliary supervision according to reconstruction difficulty, encouraging the model to focus more on hard-to-reconstruct modalities and samples.

MCE [38] optimizes training dynamics via game-theoretic evaluations and promotes semantic robustness through subset prediction, thereby encouraging balanced feature capability even under highly imbalanced missing rates.

Gradient-Based and Other Approaches. This group consists of methods that do not directly model missingness or imbalance, but instead rely on optimization-level techniques or generic multimodal fusion strategies.

OGM-GE [21] introduces orthogonal gradient modulation for pairs of modalities to reduce gradient conflict and enforces gradient

equilibrium across modalities, leading to more balanced and stable multimodal optimization.

Ada2I [20] rectifies learning imbalances by dynamically re-weighting feature and modality contributions under the supervision of a learning-discrepancy metric, so that modalities with under-optimized features receive stronger updates.

In addition, we include a **naive missing-modality baseline** that performs simple zero imputation for absent modalities, feeding zero vectors into the fusion network whenever a modality is missing. This baseline reflects the common practice of treating missing inputs as all-zero features and serves as a lower bound for more sophisticated missing-modality handling methods.

D Implementation Details

D.1 Benchmark Setup

D.1.1 Unified Configuration. The entry point of our pipeline is managed by a `ConfigManager` and a `BaseConfig` class. This structure allows for dynamic loading of model-specific configurations while maintaining a consistent interface for experimental arguments such as missing rates and hyperparameters.

To initiate an experiment, the system parses command-line arguments to select the base model and override default parameters:

Listing 1: Initialization of Configuration and Arguments

```
config_manager = ConfigManager()
args = config_manager.get_args()

# Example: Setting missing rates (Modal MR) for
#           Audio, Visual, Language
args.modal_MR = [0.5, 0.3, 0.0]
```

The `args` object above encapsulates crucial settings, including `modal_MR` (missing rates for A/V/L modalities), `dataset_mode` (Conversational or Non-conversational) and other optimization hyperparameters.

D.1.2 Data Loading Protocol. We provide a unified `create_dataset` interface that abstracts the complexity of different datasets (e.g., IEMOCAP, CMU-MOSI). The data loader automatically handles the generation of missing modality masks based on the specified protocols. Listing 2 describes detail of unified data loading interface.

Inside the `DataLoader` class, specific masking protocol (SMR or IMR) is applied to simulate missing modalities. The loader returns a dictionary containing aligned features (`A_feat`, `V_feat`, `L_feat`) and their corresponding availability masks.

D.1.3 Model Construction. To evaluate diverse architectures fairly, we wrap all models within a generic `Model` class. This wrapper dynamically instantiates the specific encoder and base model logic defined in the configuration. Beyond instantiation, it provides a standardized interface for loss computation and advanced optimization strategies. Details can be seen in Listing 3.

D.1.4 Training and Evaluation. The `train.py` pipeline is designed to be model-agnostic (Algorithm 1), incorporating two independent evaluation modules (MEI and MLI). It also standardizes the calculation of key performance metrics, including Weighted Accuracy (WA), Unweighted Accuracy (UA), and F1-score.

Listing 2: Unified Data Loading Interface

```

def create_dataset(args):
    # Dynamically load dataset library (
    # Conversational or Non-con)
    lib = find_dataset_using_name(args.
        dataset_mode)

    # Load raw data and generate missing
    # masks
    dataset, dims = lib.load_data(
        args.data_dir, args.dataset, args.
        modal_MR
    )

    # Common arguments for all data loaders
    loader_args = {
        'batch_size': args.batch_size,
        'embedding_dim': dims,
        'regression': args.regression,
        'batch_first': args.batch_first,
        'device': args.device
    }

    # Initialize PyTorch DataLoaders
    train_loader = lib.DataLoader(dataset['
        train'], **loader_args)
    valid_loader = lib.DataLoader(dataset['
        valid'], **loader_args)
    test_loader = lib.DataLoader(dataset['
        test'], **loader_args)

    return [train_loader, valid_loader,
        test_loader], dims

```

D.2 Experimental Setup

For all baselines, we adopt their official implementations, except for OGM-GE, for which a variant capable of handling three modalities is employed. Our benchmark is implemented in PyTorch¹ and experiment tracking is conducted using Comet.ml². All experiments are run on a Tesla T4 GPU, and the final results are averaged over five runs with different random seeds. For consistency, all methods are trained under the same optimization budget and unified training and logging configurations across all datasets. Specifically, we use batch_size=16 for conversational handling methods and batch_size=128 for non-conversational handling methods, with epochs=50, early_stop=10, the Adam optimizer, and a learning rate of 2e-4.

E Additional Experiment Results

E.1 Full SMR and IMR Results on All Datasets

We provide the complete SMR/IMR results for all benchmarks to complement the main-text tables. Table 7 reports performance on CMU-MOSEI across different missing-rate configurations, while Table 8 presents the corresponding results on CH-SIMS.

¹<https://pytorch.org/>

²<https://comet.ml>

Listing 3: Model Interface

```

class Model(nn.Module):
    def __init__(self, args):
        super(Model, self).__init__()
        # Dynamically find encoder and
        # specific multimodal method
        base_encoder = find_encoder(args)
        base_model = find_basemodel(args)

        self.base_model = base_model(args,
            base_encoder)
        # Select loss function based on task
        # type
        self.task_loss = MaskedMSELoss(args)
        if args.regression else
            MaskedCELoss(args)

    def forward(self, inputs):
        self.set_input(inputs) # Unpack
        # targets and masks
        return self.base_model.get_outputs()

    def get_loss(self, outputs):
        # Calculate primary task loss
        # considering the valid mask (umask
        # )
        loss = {
            'task_loss': self.task_weight *
                self.task_loss(outputs[0],
                    self.target, self.umask)
        }

        # Aggregate auxiliary losses from the
        # specific base model
        sub_loss = self.base_model.get_loss(
            outputs)
        for k in sub_loss:
            loss[k] = sub_loss[k]

        return loss

    def apply_modulation(self, outputs):
        # Hook for gradient-based method (e.g
        # ., OGM, Ada2I)
        self.base_model.apply_modulation(
            outputs)

```

Table 9 summarizes the performance on IEMOCAP under varying imbalanced missing rates, and Table 10 shows the results on CMU-MOSI. These tables give a complete view of how all baselines and our method behave under both symmetric and imbalanced missing-modality regimes on each dataset.

To better understand modality imbalance and optimization behavior, we report additional MEI/MLI statistics and training-time measurements. Table 11 summarizes MEI_{UA}/MLI (%) on CMU-MOSEI for representative methods from each family, quantifying how severely different approaches suffer from modality imbalance during training.

Additionally, we report ablation about under different bimodal combinations on non missing data (Table 12).

Table 7: Performance comparison on CMU-MOSEI

Method	Setting	0.3 / (0.1, 0.2, 0.6)			0.5 / (0.2, 0.5, 0.8)			0.7 / (0.4, 0.8, 0.9)		
		Acc-2(↑)	MAE(↓)	Corr(↑)	Acc-2(↑)	MAE(↓)	Corr(↑)	Acc-2(↑)	MAE(↓)	Corr(↑)
MMIN	SMR	77.72±0.47	0.748±0.022	0.641±0.014	73.64±2.82	0.814±0.015	0.558±0.004	69.60±1.42	0.891±0.032	0.447±0.041
	IMR	71.80±0.50	0.855±0.021	0.497±0.026	68.97±0.27	0.890±0.005	0.427±0.010	68.00±0.36	0.916±0.002	0.392±0.011
GCNet	SMR	80.22±1.10	0.706±0.024	0.692±0.023	76.84±0.67	0.773±0.016	0.621±0.018	76.34±0.96	0.781±0.014	0.599±0.016
	IMR	76.74±0.86	0.776±0.016	0.616±0.016	73.89±0.45	0.828±0.010	0.541±0.019	73.19±0.63	0.839±0.013	0.525±0.021
RedCore	SMR	77.20±0.52	0.760±0.007	0.631±0.009	72.57±0.79	0.845±0.012	0.535±0.015	68.10±0.44	0.902±0.012	0.443±0.014
	IMR	70.39±0.54	0.866±0.006	0.491±0.010	66.45±0.53	0.932±0.009	0.381±0.010	65.87±0.49	0.951±0.006	0.352±0.018
MCE	SMR	77.87±0.64	0.746±0.020	0.647±0.009	73.21±0.76	0.832±0.016	0.536±0.020	69.71±1.04	0.885±0.024	0.448±0.033
	IMR	72.25±0.79	0.846±0.009	0.513±0.010	67.32±0.48	0.920±0.004	0.391±0.001	67.73±0.12	0.928±0.003	0.373±0.010
Ada2I	SMR	82.56±0.39	0.845±0.070	0.718±0.012	80.13±0.32	0.940±0.112	0.680±0.004	78.36±0.47	0.873±0.054	0.624±0.012
	IMR	78.96±0.44	0.917±0.080	0.646±0.005	75.25±0.41	0.920±0.035	0.573±0.012	74.51±0.91	0.910±0.030	0.541±0.034
OGM-GE	SMR	82.00±0.39	0.683±0.023	0.710±0.018	79.69±0.22	0.736±0.012	0.660±0.005	76.79±0.35	0.790±0.011	0.600±0.010
	IMR	77.72±0.58	0.767±0.006	0.624±0.004	74.24±0.37	0.835±0.003	0.527±0.004	74.13±0.55	0.850±0.021	0.523±0.018

Table 8: Performance comparison on CH-SIMS

Method	Setting	0.3 / (0.1, 0.2, 0.6)			0.5 / (0.2, 0.5, 0.8)			0.7 / (0.4, 0.8, 0.9)		
		Acc-2(↑)	MAE(↓)	Corr(↑)	Acc-2(↑)	MAE(↓)	Corr(↑)	Acc-2(↑)	MAE(↓)	Corr(↑)
MMIN	SMR	78.19±0.26	0.480±0.012	0.596±0.026	72.21±1.86	0.544±0.009	0.485±0.028	67.26±2.28	0.594±0.034	0.330±0.097
	IMR	71.80±0.50	0.509±0.010	0.542±0.031	68.97±0.27	0.621±0.046	0.212±0.190	68.00±0.36	0.603±0.013	0.318±0.036
GCNet	SMR	66.03±0.59	0.628±0.008	0.234±0.024	65.97±1.45	0.645±0.010	0.168±0.041	65.10±0.66	0.644±0.005	0.163±0.022
	IMR	64.94±0.96	0.648±0.009	0.161±0.055	64.77±0.67	0.648±0.002	0.152±0.026	65.55±0.43	0.649±0.002	0.140±0.024
RedCore	SMR	75.25±1.57	0.517±0.024	0.550±0.053	70.82±1.49	0.561±0.012	0.445±0.023	66.95±1.39	0.596±0.016	0.354±0.040
	IMR	76.28±0.63	0.521±0.008	0.538±0.008	66.15±1.60	0.591±0.011	0.355±0.037	64.34±0.12	0.613±0.006	0.304±0.021
MCE	SMR	77.06±0.81	0.486±0.006	0.581±0.027	73.09±0.68	0.528±0.013	0.498±0.023	67.78±1.83	0.590±0.021	0.359±0.033
	IMR	74.39±1.68	0.514±0.009	0.521±0.024	67.44±3.40	0.578±0.023	0.372±0.061	68.47±0.85	0.582±0.019	0.350±0.028
Ada2I	SMR	61.08±3.45	0.728±0.059	0.179±0.062	58.55±3.35	0.800±0.105	0.086±0.036	59.74±4.66	0.996±0.388	0.084±0.087
	IMR	60.30±1.67	1.028±0.190	0.111±0.019	63.31±1.43	0.755±0.123	0.156±0.080	58.59±3.16	1.228±0.379	0.026±0.058
OGM-GE	SMR	77.16±1.08	0.539±0.007	0.506±0.013	72.06±0.35	0.572±0.005	0.422±0.028	65.67±1.43	0.647±0.011	0.191±0.032
	IMR	69.07±1.38	0.624±0.019	0.281±0.065	66.58±1.55	0.634±0.020	0.202±0.088	65.63±1.90	0.654±0.020	0.111±0.104

Table 9: Performance comparison on IEMOCAP under different imbalanced missing rates

Method	(0.1, 0.6, 0.2)		(0.6, 0.1, 0.2)		(0.2, 0.8, 0.5)		(0.8, 0.2, 0.5)		(0.4, 0.9, 0.8)		(0.9, 0.4, 0.8)	
	WA	F1										
MMIN	66.04±2.63	66.34±2.60	68.95±0.65	69.05±0.69	57.31±0.88	57.46±0.89	60.35±1.61	60.22±1.26	52.32±2.17	52.38±2.09	53.72±0.50	53.74±0.46
GCNet	74.61±2.28	74.91±2.04	77.14±2.63	76.87±2.94	68.03±4.52	68.31±4.45	76.52±2.09	76.33±2.12	65.24±0.56	65.58±0.43	72.52±3.67	72.42±3.43
RedCore	65.94±0.27	66.11±0.25	65.94±0.56	66.12±0.57	60.05±0.74	60.27±0.72	59.97±2.73	60.06±2.40	52.61±1.42	52.52±1.49	53.34±2.46	53.56±2.35
MCE	68.73±0.84	68.84±0.81	69.54±0.62	69.49±0.55	59.54±1.20	59.67±1.25	62.47±0.89	62.46±0.77	53.93±0.81	53.92±0.86	55.43±1.55	55.18±1.47
Ada2I	80.12±1.03	80.31±0.98	77.89±0.53	78.00±0.47	76.92±1.73	77.14±1.69	74.48±1.22	74.36±1.38	73.70±2.12	73.62±2.74	71.60±2.68	71.32±3.10
OGM-GE	71.39±5.20	71.57±5.28	74.80±1.64	74.89±1.49	69.83±2.83	69.92±2.76	72.81±2.17	72.88±1.98	66.04±1.32	66.48±1.26	64.22±5.56	63.57±6.46

E.2 MEI/MLI Analysis and Training Cost

Figure 8 further tracks MEI over epochs for GCNet on IEMOCAP under different task-specific metrics (UA/WA/F1), revealing the temporal evolution of imbalance. Finally, Figure 7 compares the

estimated training time per epoch of all baselines, providing a complementary view of their computational cost alongside performance.

Algorithm 1 Benchmark Training Pipeline

```

1: Input: args, train_loader, val_loader, test_loader
2: Initialize: model, optimizer, scheduler
3: Initialize Analyzers:  $\mathcal{A}_{MLI}$  (if enabled),  $\mathcal{A}_{MEI}$  (if enabled)
4: for epoch  $\leftarrow$  1 to args.epochs do
5:   model.train()
6:   for batch in train_loader do
7:     outputs  $\leftarrow$  model(batch)
8:     loss  $\leftarrow$  model.get_loss(outputs)
9:     if  $\mathcal{A}_{MLI}$  is enabled then
10:       $\mathcal{A}_{MLI}.step\_evaluate(model, outputs, batch)$ 
11:     end if
12:     loss.backward()
13:     model.clip_gradients(args.max_grad_norm)
14:     if args.modulation is active then
15:       model.apply_modulation(outputs)
16:     end if
17:     optimizer.step()
18:   end for
19:   val_metrics  $\leftarrow$  evaluate(args, model, val_loader)
20:   scheduler.step()
21:   if  $\mathcal{A}_{MEI}$  is enabled and epoch%MEI_epoch == 0 then
22:      $\mathcal{A}_{MEI}.evaluate(model, val_loader)$ 
23:   end if
24:   if val_metrics is best then
25:     Save checkpoint state  $\theta^*$ 
26:   end if
27:   Check Early Stopping
28: end for
29: Test Phase:
30: Load best model state  $\theta^*$ 
31: test_metrics  $\leftarrow$  test(args, model, test_loader)
32: Final Analysis:
33: if  $\mathcal{A}_{MLI}$  is enabled then  $\mathcal{A}_{MLI}.evaluate()$ 
34: end if
35: if  $\mathcal{A}_{MEI}$  is enabled then  $\mathcal{A}_{MEI}.evaluate(model, test_loader)$ 
36: end if

```

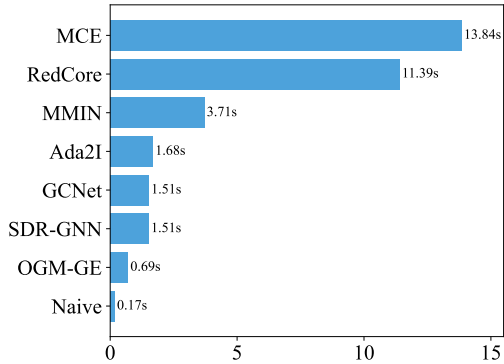


Figure 7: Estimated training time (sec/epoch) of the baselines.

Table 10: Performance comparison on CMU-MOSI under different imbalanced missing rates

Method	Setting	Acc-2(\uparrow)	MAE(\downarrow)	Corr(\uparrow)
MMIN	(0.1,0.6,0.2)	74.13 \pm 0.72	1.009 \pm 0.019	0.635 \pm 0.010
	(0.6,0.1,0.2)	73.73 \pm 0.96	1.076 \pm 0.097	0.622 \pm 0.022
	(0.2,0.8,0.5)	67.02 \pm 0.94	1.191 \pm 0.024	0.514 \pm 0.001
	(0.8,0.2,0.5)	65.65 \pm 0.31	1.210 \pm 0.028	0.493 \pm 0.006
	(0.4,0.9,0.8)	52.03 \pm 7.26	1.397 \pm 0.077	0.263 \pm 0.166
GCNet	(0.1,0.6,0.2)	70.78 \pm 0.61	1.157 \pm 0.017	0.507 \pm 0.017
	(0.6,0.1,0.2)	70.73 \pm 1.14	1.146 \pm 0.017	0.516 \pm 0.014
	(0.2,0.8,0.5)	66.15 \pm 0.89	1.285 \pm 0.026	0.403 \pm 0.016
	(0.8,0.2,0.5)	64.99 \pm 1.24	1.293 \pm 0.028	0.386 \pm 0.017
	(0.4,0.9,0.8)	61.83 \pm 1.34	1.330 \pm 0.025	0.314 \pm 0.010
RedCore	(0.1,0.6,0.2)	74.03 \pm 1.50	1.072 \pm 0.023	0.578 \pm 0.004
	(0.6,0.1,0.2)	74.84 \pm 1.74	1.076 \pm 0.030	0.593 \pm 0.010
	(0.2,0.8,0.5)	65.95 \pm 0.61	1.234 \pm 0.010	0.461 \pm 0.009
	(0.8,0.2,0.5)	67.02 \pm 1.18	1.209 \pm 0.011	0.480 \pm 0.007
	(0.4,0.9,0.8)	60.41 \pm 1.00	1.364 \pm 0.006	0.355 \pm 0.013
MCE	(0.1,0.6,0.2)	74.54 \pm 1.40	1.049 \pm 0.039	0.613 \pm 0.013
	(0.6,0.1,0.2)	73.93 \pm 0.69	1.049 \pm 0.018	0.611 \pm 0.011
	(0.2,0.8,0.5)	66.41 \pm 1.22	1.200 \pm 0.015	0.491 \pm 0.011
	(0.8,0.2,0.5)	66.26 \pm 1.83	1.208 \pm 0.030	0.500 \pm 0.023
	(0.4,0.9,0.8)	59.60 \pm 2.07	1.324 \pm 0.010	0.383 \pm 0.006
Ada2I	(0.1,0.6,0.2)	71.29 \pm 4.56	1.416 \pm 0.134	0.562 \pm 0.043
	(0.6,0.1,0.2)	73.47 \pm 3.14	1.210 \pm 0.091	0.557 \pm 0.059
	(0.2,0.8,0.5)	66.41 \pm 1.15	1.310 \pm 0.061	0.442 \pm 0.017
	(0.8,0.2,0.5)	62.24 \pm 2.61	1.341 \pm 0.032	0.382 \pm 0.017
	(0.4,0.9,0.8)	49.08 \pm 4.04	1.724 \pm 0.202	0.118 \pm 0.082
OGM-GE	(0.1,0.6,0.2)	71.85 \pm 1.27	1.156 \pm 0.027	0.537 \pm 0.015
	(0.6,0.1,0.2)	71.74 \pm 0.38	1.151 \pm 0.022	0.531 \pm 0.015
	(0.2,0.8,0.5)	65.39 \pm 2.24	1.290 \pm 0.032	0.391 \pm 0.054
	(0.8,0.2,0.5)	64.17 \pm 1.95	1.323 \pm 0.046	0.358 \pm 0.072
	(0.4,0.9,0.8)	52.23 \pm 8.15	1.432 \pm 0.082	0.116 \pm 0.176
	(0.9,0.4,0.8)	51.42 \pm 7.23	1.440 \pm 0.069	0.125 \pm 0.175

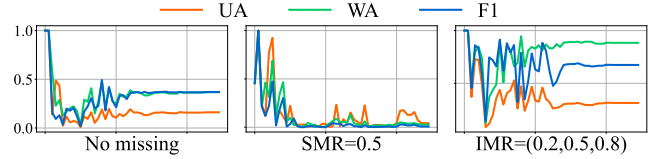


Figure 8: MEI evaluated by different task-specific metrics UA/WA/F1 during the training of GCNet on IEMOCAP.

E.3 Case Studies: Modality Contribution and Gradient Dynamics

We further conduct case studies to analyze how representative methods behave at the modality and optimization level.

Table 11: MEI_{UA}/MLI(%) of representatives from each method-family on CMU-MOSEI.

Method	Setting	0.3 / (0.1, 0.2, 0.6)		0.5 / (0.2, 0.5, 0.8)		0.7 / (0.4, 0.8, 0.9)	
		MEI _{UA}	MLI	MEI _{UA}	MLI	MEI _{UA}	MLI
GCNet	SMR	74.25 \pm 8.58	33.63 \pm 2.97	82.90 \pm 7.13	41.05 \pm 1.84	89.51 \pm 7.02	44.12 \pm 3.99
	IMR	62.83 \pm 15.95	32.86 \pm 3.65	63.82 \pm 6.30	37.65 \pm 2.67	74.61 \pm 15.01	39.74 \pm 2.49
RedCore	SMR	80.19 \pm 2.73	33.92 \pm 1.27	80.52 \pm 4.42	38.63 \pm 2.29	83.62 \pm 0.75	43.25 \pm 2.43
	IMR	80.65 \pm 1.39	35.00 \pm 2.10	84.36 \pm 3.72	40.40 \pm 3.51	84.83 \pm 1.73	42.86 \pm 4.67
Ada2I	SMR	86.82 \pm 5.45	15.22 \pm 1.21	80.65 \pm 10.39	13.41 \pm 2.22	89.86 \pm 7.60	12.79 \pm 1.48
	IMR	81.72 \pm 10.60	14.91 \pm 1.53	77.97 \pm 13.79	14.41 \pm 1.19	81.27 \pm 13.01	12.21 \pm 0.56

Table 12: Performance comparison under different bimodal combinations (A: Audio, V: Visual, L: Language) on non-missing data

Method	AV			AL			VL		
	WA	F1	MEI _{UA}	WA	F1	MEI _{UA}	WA	F1	MEI _{UA}
GCNet	68.61 \pm 1.92	69.19 \pm 1.56	35.05 \pm 21.01	74.62 \pm 2.71	74.83 \pm 2.75	6.80 \pm 6.16	78.31 \pm 1.40	78.04 \pm 1.26	62.24 \pm 20.04
RedCore	72.93 \pm 0.95	72.89 \pm 0.92	13.75 \pm 1.39	80.61 \pm 2.18	80.84 \pm 2.09	8.62 \pm 7.84	78.69 \pm 2.85	78.50 \pm 2.94	39.77 \pm 29.06
Ada2I	62.34 \pm 0.67	62.47 \pm 0.74	9.55 \pm 6.20	65.51 \pm 1.49	65.53 \pm 1.57	71.70 \pm 14.28	68.73 \pm 0.74	68.73 \pm 0.64	45.48 \pm 19.01

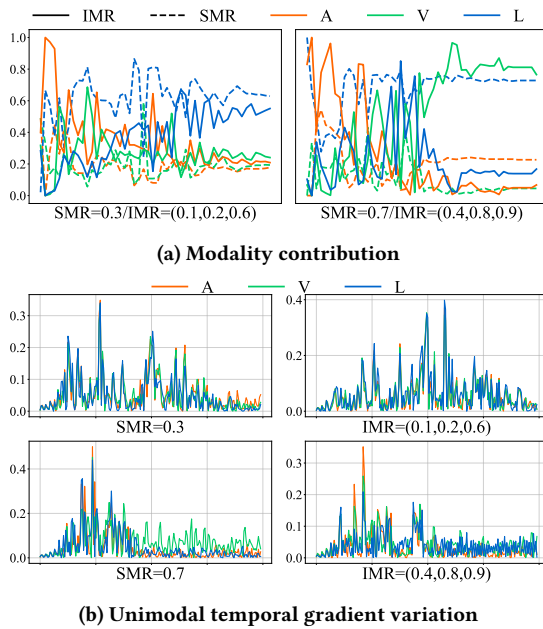


Figure 9: Diagnosis of GCNet on a different IEMOCAP train/valid split from Figure 5.

For IEMOCAP, Figures 9 and 10 visualize modality contribution and unimodal temporal gradient variation for GCNet and RedCore, while Figure 11 presents the same diagnostics for Ada2I.

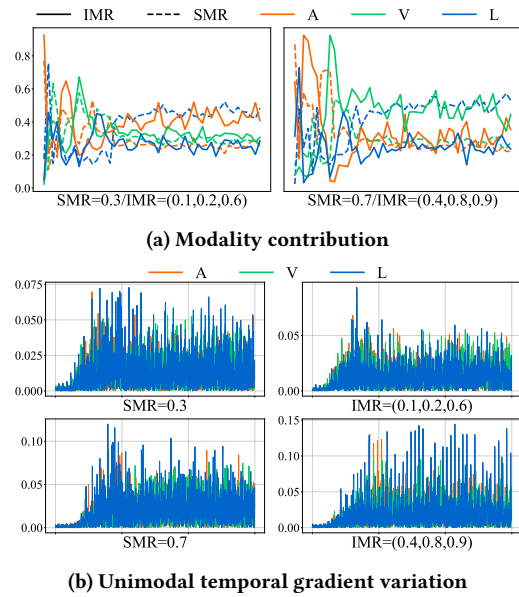
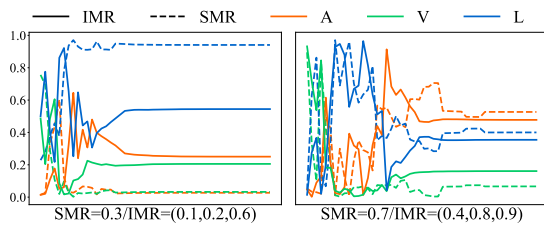
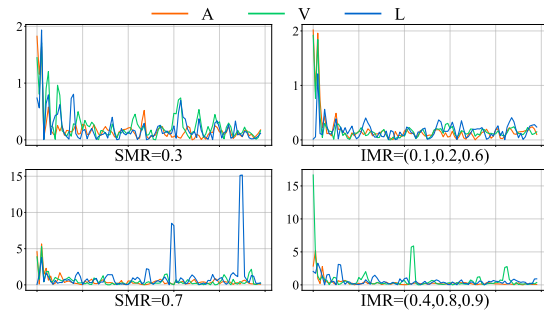


Figure 10: Diagnosis of RedCore on IEMOCAP.

For CMU-MOSI, Figures 14, 12, and 13 provide analogous plots for GCNet, RedCore, and Ada2I, respectively. These qualitative results complement the quantitative tables by revealing how different architectures redistribute modality contributions and stabilize (or destabilize) gradients under imbalanced missing rates.

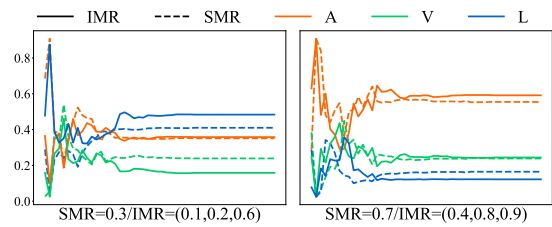


(a) Modality contribution

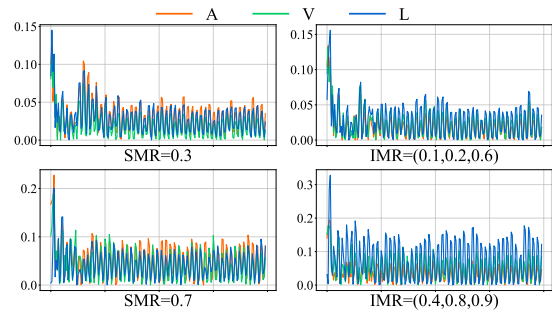


(b) Unimodal temporal gradient variation

Figure 13: Diagnosis of Ada2I on CMU-MOSI.

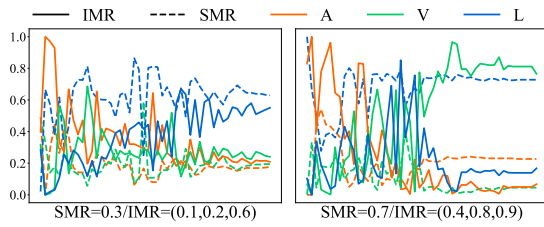


(a) Modality contribution

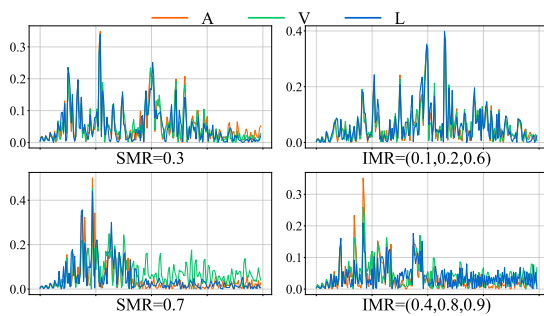


(b) Unimodal temporal gradient variation

Figure 11: Diagnosis of Ada2I on IEMOCAP.

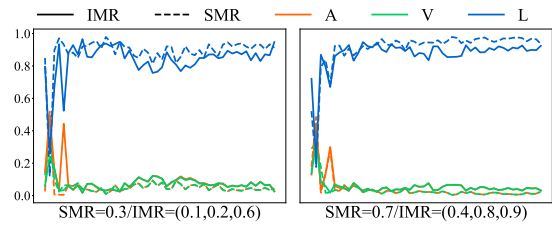


(a) Modality contribution

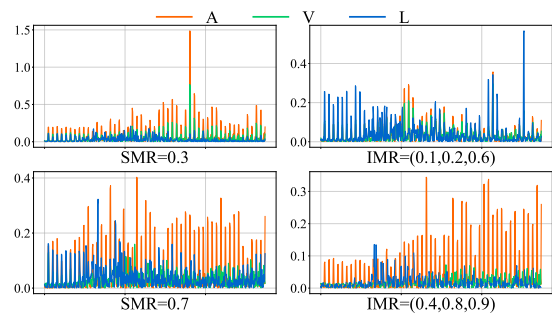


(b) Unimodal temporal gradient variation

Figure 14: Diagnosis of GCNet on CMU-MOSI.



(a) Modality contribution



(b) Unimodal temporal gradient variation

Figure 12: Diagnosis of RedCore on CMU-MOSI.